

**The selezipag active metabolite ACT-333679 displays strong anti-contractile and anti-remodeling effects, but low  $\beta$ -arrestin recruitment and desensitization potential**

John Gatfield <sup>#</sup>, Katalin Menyhart, Daniel Wanner, Carmela Gnerre, Lucile Monnier, Keith Morrison, Patrick Hess, Marc Iglarz, Martine Clozel and Oliver Nayler

Actelion Pharmaceuticals Ltd, Allschwil, Switzerland

**Running title:** Efficacy and desensitization profile of selexipag

**Corresponding author:** John Gatfield

Actelion Pharmaceuticals Ltd

Gewerbestrasse 16

4123 Allschwil

Switzerland

+41 61 565 63 35 (phone)

+41 61 565 89 02 (fax)

john.gatfield@actelion.com

Text pages: 44

Number of tables: 4

Number of figures: 11

Number of references: 43

Abstract: 235 words

Introduction: 605 words

Discussion: 982 words

Recommended section assignment: Cardiovascular

**Abbreviations:**

ACT-333679 or MRE-269, {4-[(5,6-diphenylpyrazin-2-yl)(isopropyl)amino]butoxy}acetic acid; AT<sub>1</sub>, angiotensin receptor type 1; BSA, bovine serum albumin; CHO, Chinese hamster ovary; DTT, dithiothreitol; EC<sub>50</sub>, concentration leading to half-maximal stimulation; ECM, extracellular matrix; E<sub>max</sub>, maximal efficacy; EP<sub>1</sub> receptor, prostaglandin E<sub>2</sub> receptor type 1; ET-1, endothelin-1; FBS, fetal bovine serum; GPCR, G protein-coupled receptor; h, human; HBSS, Hank's balanced salt solution; HEK, human embryonic kidney; HEPES, 4-(2-

hydroxyethyl)-1-piperazineethanesulfonic acid; IBMX, 3-Isobutyl-1-methylxanthine; IP receptor, prostaglandin I<sub>2</sub> receptor; LC/MS, high-performance liquid chromatography coupled to mass spectrometry; MAP, mean arterial blood pressure; MCT, monocrotaline; MLC, myosine light chain; MLCK, myosin light chain kinase; MPAP, mean pulmonary arterial blood pressure; PAH, pulmonary arterial hypertension; PASMC, pulmonary arterial smooth muscle cells; PDGF, platelet-derived growth factor; PGI<sub>2</sub>, prostaglandin I<sub>2</sub> or prostacyclin; PH, pulmonary hypertension; PMSF, phenylmethylsulfonylfluoride; selexipag, 2-{4-[(5,6-diphenylpyrazin-2-yl)(isopropyl)amino]butoxy}-*N*-(methylsulfonyl)acetamide; SD, standard deviation; SEM, standard error of the mean; SHR, spontaneously hypertensive rats; S1P1, sphingosine-1-phosphate receptor type 1

## ABSTRACT

Prostacyclin (PGI<sub>2</sub>) receptor (IP receptor) agonists, which are indicated for the treatment of pulmonary arterial hypertension (PAH), increase cytosolic cAMP levels and thereby inhibit pulmonary vasoconstriction, pulmonary arterial smooth muscle cell (PASMC) proliferation and extracellular matrix synthesis. Selexipag (Uptravi®) is the first non-prostanoid IP receptor agonist, it is available orally and was recently approved for the treatment of PAH. In this study we show that the active metabolite of selexipag and the main contributor to clinical efficacy, ACT-333679 (previously known as MRE-269), behaved as full agonist in multiple PAH-relevant receptor-distal - or downstream cellular assays with a maximal efficacy comparable to that of the prototypic PGI<sub>2</sub> analog iloprost: In PASMC, ACT-333679 potently induced cellular relaxation (EC<sub>50</sub>=4.3 nM), inhibited cell proliferation (IC<sub>50</sub>=4.0 nM) as well as extracellular matrix synthesis (IC<sub>50</sub>=8.3 nM). In contrast, ACT-333679 displayed partial agonism in receptor-proximal - or upstream - cAMP accumulation assays (E<sub>max</sub>=56%) when compared to iloprost and the PGI<sub>2</sub> analogs beraprost and treprostinil (E<sub>max</sub>~100%). Partial agonism of ACT-333679 also resulted in limited β-arrestin recruitment (E<sub>max</sub>=40%) and lack of sustained IP receptor internalization, whereas all tested PGI<sub>2</sub> analogs behaved as full agonists in these desensitization-related assays. In line with these *in vitro* findings, selexipag, but not treprostinil, displayed sustained efficacy in rat models of pulmonary and systemic hypertension. Thus, the partial agonism of ACT-333679 allows for full efficacy in amplified receptor-distal PAH-relevant readouts while causing limited activity in desensitization-related receptor-proximal readouts.

## INTRODUCTION

Prostacyclin ( $\text{PGI}_2$ ) is an arachidonic acid metabolite synthesized mainly through endothelial cells by cyclooxygenase enzymes in conjunction with  $\text{PGI}_2$  synthase.  $\text{PGI}_2$  serves as an autocrine/paracrine mediator, modulating various physiological processes by binding and activating the prostacyclin receptor (IP receptor), a G-protein coupled receptor (GPCR) that stimulates adenylate cyclase to synthesize cyclic AMP (cAMP) (Boie et al., 1994). The IP receptor is highly expressed in cell types such as vascular smooth muscle cells, fibroblasts, platelets and leucocytes. Insufficient  $\text{PGI}_2$  synthesis and IP receptor signaling have been linked to cardiovascular pathologies, especially pulmonary arterial hypertension (PAH) (Christman et al., 1992; Tuder et al., 1999; Arehart et al., 2008). PAH is a rare disease characterized by increased pressure in the pulmonary circulation caused by constriction and progressive remodeling of the pulmonary vasculature and thus increased pulmonary vascular resistance (Galie et al., 2009; Morrell et al., 2009). Exogenous supplementation of synthetic  $\text{PGI}_2$  (epoprostenol) by continuous intravenous (i.v.) application was the first efficacious therapy in PAH (Barst et al., 1996).

Currently, three  $\text{PGI}_2$  analogs have been marketed for treatment of PAH: iloprost, treprostinil and beraprost (Olschewski et al., 2004). Several limitations of  $\text{PGI}_2$  analog therapy are known: they are not selective, i.e. they activate other prostanoid receptors, and they display chemical and metabolic instability limiting their potential for oral administration (Kuwano et al., 2007; Whittle et al., 2012). In addition, being GPCR agonists, it has been suggested that  $\text{PGI}_2$  analogs might have the potential to cause tachyphylaxis (Rubin et al., 1990; Archer et al., 1996; Shapiro et al., 1997; Barst et al., 2003) making it necessary to escalate drug dosing over time. Tachyphylaxis can be caused by different mechanisms. In the case of  $\text{PGI}_2$  and its analogs, one of the main mechanisms is thought to be classical receptor internalization into the endocytic compartment (Hasse et al., 2003; Smyth et al., 2003; Smyth et al., 2000; Reid et al., 2010).

In order to overcome the aforementioned pharmacological limitations associated with PGI<sub>2</sub> structures, Actelion/Nippon Shinyaku have developed a selective, oral non-prostanoid IP receptor agonist, selexipag (2-{4-[(5,6-diphenylpyrazin-2-yl)(isopropyl)amino]butoxy}-*N*-(methylsulfonyl)acetamide, previously known as NS-304) (Asaki et al., 2015), which has been recently approved in the US, the EU and Japan for the treatment of PAH (Sitbon et al., 2015). After systemic absorption, selexipag, the parent drug, is hydrolyzed to the highly potent metabolite ACT-333679 ({4-[(5,6-diphenylpyrazin-2-yl)(isopropyl)amino]butoxy}acetic acid, previously known as MRE-269), the major driver of clinical efficacy (Figure 1) (Kuwano et al., 2007; Kuwano et al., 2008). ACT-333679 differentiates favorably from PGI<sub>2</sub> analogs in terms of its higher metabolic stability and its high IP receptor selectivity. To date, the *in vitro* activities of selexipag and in particular its active metabolite, ACT-333679, using PAH-relevant assays in PASMC have not been reported. Furthermore, it is currently not known how ACT-333679 compares with PGI<sub>2</sub> analogs regarding its IP receptor internalizing and desensitizing properties.

In the present study we compared the activity of ACT-333679 with that of the prototypic PGI<sub>2</sub> analog iloprost by measuring diverse PAH-relevant parameters in PASMC such as cellular relaxation, proliferation and extracellular matrix synthesis and found both compounds to be full agonists. We then uncovered unique partial agonism of ACT-333679 in receptor proximal readouts such as induction of cAMP synthesis, recruitment of  $\beta$ -arrestin and IP receptor internalization. This partial agonism is in contrast to the full agonism displayed by iloprost and other PGI<sub>2</sub> analogs (beraprost, treprostinil). Finally, the propensity of IP receptor agonists to induce tachyphylaxis was tested *in vivo* comparing selexipag with the PGI<sub>2</sub> analog treprostinil. Our data suggest that the unique partial agonism exhibited by ACT-333679 on receptor-proximal parameters reduces its potential for desensitization, while still reaching maximal effects on downstream parameters relevant to PAH.

## MATERIALS AND METHODS

**Compounds.** Selexipag and ACT-333679 were synthesized by Nippon Shinyaku Co. Ltd (Kyoto, Japan). Beraprost, iloprost and treprostinil were purchased from Cayman Chemical (Ann Arbor, MI, USA).

**Cell culture.** For use in immunofluorescence microscopy, CHO-K1 cells expressing the human IP receptor (CHO-hIP) were cultured in Ham's F12 containing 10 % FBS heat-inactivated (Brunschwig, Basel, Switzerland), 100 U/ml penicillin, 100 µg/ml streptomycin, and 600 µg/ml geneticin (Life Technologies, Zug, Switzerland). CHO-hIP PathHunter® cells for beta-arrestin assays (DiscoverX, Birmingham, UK) were cultured in Ham's F12 containing 10 % FBS heat-inactivated, 100 U/ml penicillin, 100 µg/ml streptomycin, 300 µg/ml hygromycin (Life Technologies, Zug, Switzerland) and 800 µg/ml geneticin.

The human IP receptor-expressing cell pool T-REx<sup>TM</sup>-HEK-293-CMV.TO.FLAG-humanIP-C9 (abbreviated T-REx-HEK-hIP) was generated by integrase-mediated homologous recombination of the IP receptor sequence into the T-REx<sup>TM</sup> HEK293 background. This expression system allows the tetracycline-inducible expression of genes of interest from one defined insertion site and the generated cells were used (i) in cAMP experiments to evaluate cAMP responses to IP receptor agonists at high and low expression levels and (ii) in flow cytometry to observe agonist-induced IP receptor internalization. Parental T-REx<sup>TM</sup>-HEK293 cells (Life Technologies, Zug, Switzerland) were cultivated in growth medium (DMEM + GlutaMAX<sup>TM</sup>-I (Life Technologies, Zug, Switzerland), 10 % dialyzed FBS (Life Technologies, Zug, Switzerland), 100 U/mL penicillin, 100 µg/mL streptomycin, 0.1 mg/ml hygromycin B (Life Technologies, Zug, Switzerland), 5 µg/ml blasticidin (Life Technologies, Zug, Switzerland) and 1 % non-essential amino acid solution (Life Technologies, Zug, Switzerland)). Recombinant T-REx-HEK-hIP cells were cultivated in selection medium (growth medium containing 1 mg/ml Geneticin (Life Technologies, Zug,

Switzerland) instead of hygromycin. Every second day the medium was exchanged with fresh selection medium.

Human proximal pulmonary arterial smooth muscle cells (PASMC) (Cat.No.CC-2581 LotNo.0000200208, male, Lonza, Basel, Switzerland) were cultivated and propagated in complete cell growth medium (SmBM, supplemented with SmGM-2 SingleQuots (0.2 % hEGF, 0.1 % insulin, 0.2 % hFGF-B, 5 % FBS and 0.1 % gentamicin/amphotericin-B (Lonza, Basel, Switzerland)) up to passage 4. For measurements related to proliferation and extracellular matrix synthesis ( $[^3\text{H}]$ -thymidine incorporation, p27(Kip1) and cyclin D1 immunoblotting,  $[^3\text{H}]$ -proline incorporation) cells were kept in this proliferation medium. For measurements related to shape change (impedance, tomographic microscopy, cAMP and MLCK phosphorylation), cells were treated for 48 h with differentiation medium (SmBM with 4 % FBS heat-inactivated (Brunschwig, Basel, Switzerland), 100  $\mu\text{g/mL}$  heparin sodium salt (Tocris, Zug, Switzerland), 100  $\mu\text{g/mL}$  penicillin/streptomycin (Life Technologies, Zug, Switzerland)). Heparin induces differentiation of vascular smooth muscle cells to the contractile phenotype characterized by a mature contractile apparatus (Beamish et al., 2010). Prior to stimulation with IP receptor agonists, differentiation or growth factors, cells were brought into the quiescent state by cultivation in starvation medium (SmBM, 20 mM HEPES 100  $\mu\text{g/mL}$  penicillin/streptomycin (Life Technologies, Zug, Switzerland), 0.1 % BSA, fatty acid-free (Calbiochem, San Diego, CA, USA)). Cells were used up to passage 4 and harvested for seeding for the various assays at approximately 90 % cell density.

**Impedance assays.** PASMC were seeded into E-plates (ACEA Biosciences, San Diego, CA, USA) at 5,000 cells/well and placed into the xCELLigance MP device (ACEA Biosciences, San Diego, CA, USA). The next day, medium was exchanged for differentiation medium. After 48 hours, cells starved for 6 hours in starvation medium and then subjected to IP receptor agonists diluted in starvation medium and further cultivated for several hours. Impedance measurements were performed during the whole experimental period. For

analysis, impedance traces were aligned at the last time point before IP receptor agonist addition, the vehicle baseline was subtracted and impedance minima within the first 3 hours after agonist addition were used to generate concentration-response curves.  $EC_{50}$  and  $E_{max}$  values were calculated with the proprietary  $IC_{50}$  witch software using the compound intrinsic curve maximum and minimum as plateau values. Compound efficacies were compared to the maximal efficacy of iloprost (100 %). For the ET-1/IP receptor agonist combination experiments, cells were prepared as above and after the starvation period were stimulated with 10 nM ET-1 (diluted in starvation medium), observed for 60 min until a response plateau was reached and then stimulated with a dilution series of ACT-333679 or iloprost in starvation medium, again followed by an observation period. For analysis, impedance traces were aligned at the last time point before ET-1 addition, the vehicle-vehicle baseline was subtracted and impedance minimum 60 min after IP receptor agonist addition were used to generate concentration-response curves.

**Tomographic microscopy.** Human PASMC were seeded into 35 mm tissue culture dishes (FluoroDish, World Precision Instruments Inc., Sarasota, FL, USA) at 15,000 cells/dish, grown overnight and then treated for 24 hours in differentiation medium. Then cells were starved for 3 hours by exchange for starvation medium with 20 mM HEPES. Dishes were then placed on the tomographic microscope (3D Explorer, NanoLive, Lausanne, Switzerland) and 3D tomographic images (z-stacks) were taken at regular intervals (2 min). Within the observation period, cells were treated with ET-1 (100 nM) for ~90 min followed by ACT-333679 (1  $\mu$ M) or vehicle. The plane with the best focus was picked from every z-stack and used to generate time lapse sequences. In order to get a smooth motion movie, the number of frames were increased by a combination of motion interpolation and frame blending. In brief, a similarity distance between pixels in different frames was defined by making use of the intensities of surrounding pixels. A motion vector was defined from the position of each pixel in frame "n" to the closest pixel in frame "n+1", based on the similarity distance. This

vector allowed a smooth interpolation which was used to increase the frame-rate from 0.2 to 60 frames per second. Further post-processing steps like noise reduction, gamma and contrast enhancement were applied to the final rendering of the video.

**Immunoblotting.** Isogenic T-REx-HEK-hIP cells were seeded at 15,000 cells/well into 96-well plates, and supplemented after attachment with different concentrations of tetracycline between 0 and 10 ng/mL to induce increasing IP receptor expression levels. After a 24 hour induction period, cells were washed with phosphate buffered saline (PBS) and then lysed on ice in 15  $\mu$ L/well of RIPA buffer (Sigma Aldrich, Buchs, Switzerland) containing 100 mM NaF, 4 mM Na-orthovanadate, 1 mM phenylmethylsulfonylfluoride (PMSF), 1 mM dithiothreitol (DTT) and 100 U/mL benzonase (Sigma Aldrich, Buchs, Switzerland). The contents of one well (15  $\mu$ L volume containing 10  $\mu$ g protein) were analyzed by SDS-PAGE and Western blotting using mouse-anti-human IP receptor monoclonal antibody 13-Q (1  $\mu$ g/ml, Santa Cruz Biotechnology Inc., Dallas, TX, USA) and HRP-coupled anti-mouse IgG secondary antibodies (GE Life Sciences, Glattbrugg, Switzerland). Membranes were treated with Western Lightning®-Enhanced Chemiluminescence Substrate (Perkin Elmer, Schwerzenbach, Switzerland), and the chemiluminescence signal was recorded and quantified using a chemiluminescence reader (LAS-4000) (Fujifilm, Tokyo, Japan) and the corresponding software (Multigauge V3.0, Fujifilm).

Human PSMC were seeded at 10,000 cells per well into 96-well plates that were pre-coated with fibronectin. The next morning the growth medium was exchanged for differentiation medium and after 48 hours cells were switched for 6 hours to starvation medium. The cells were then stimulated for 90 min at 37 °C with dilution series of IP receptor agonists (in starvation medium; +/- 100 nM ET-1; for MLCK and MLC phosphorylation) or with dilution series of IP receptor agonists for 24 hours at 37 °C (in starvation medium; +/- 50 ng/ml PDGF-BB; for cyclinD1 and p27/Kip1). Cells were lysed in RIPA buffer containing 100 mM NaF, 4 mM Na-orthovanadate, 1 mM PMSF, 1 mM DTT and 100 U/mL benzonase and

lysates were subjected to SDS-PAGE and immunoblotting using the polyclonal rabbit-anti-smooth muscle myosin light chain kinase phosphospecific antibody (Cat.No.441085G, Life Technologies, Zug, Switzerland), the polyclonal rabbit-anti-p27 Kip1, (1:100, Cat.No. 2552, Cell Signaling Technology, Danvers, MA, USA), the polyclonal rabbit-anti-cyclin D1(2 µg/ml, Cat.Nr. sc-753, Santa Cruz Biotechnology Inc., Dallas, TX, USA), or the polyclonal rabbit-anti-tubulin antibody (1:1000, Cat.No. 2148S, Cell Signaling Technology, Danvers, MA, USA) in combination with HRP-coupled anti-rabbit secondary antibodies (GE Life Sciences, Glattbrugg, Switzerland). The membranes were subjected to ECL reaction followed by signal detection and quantification in the LAS-4000 reader.

**[<sup>3</sup>H]-thymidine incorporation assays.** With this assay, DNA synthesis as a measure of cell proliferation is determined. Human PASMNC were seeded at 3,200 cells / well in 96-well plates in 100 µL/well growth medium and cultured overnight at 37°C / 5 % CO<sub>2</sub>. The plates were sealed (Breathseal) (Greiner, Loerrach, Germany) after every experimental manipulation. After 20 h the cells were cell-cycle arrested in 100 µL/well of starvation medium for 24 hours at 37 °C / 5 % CO<sub>2</sub>. Then the cells were supplemented with a dilution series of IP receptor agonists or a dilution series of DMSO (a vehicle control curve was used on every plate) and incubated for 2 hours at 37°C / 5 % CO<sub>2</sub>, followed by addition of 2.5 ng/mL or 10 ng/mL PDGF-BB diluted in PASMNC starvation medium and [<sup>3</sup>H]-thymidine (Perkin Elmer, Schwerzenbach, Switzerland) diluted in starvation medium (0.6 µCi/w, 10 µL/well). Cells were incubated for 24 h at 37 °C / 5 % CO<sub>2</sub>. Several control wells per plate were not treated with PDGF-BB for the determination of basal [<sup>3</sup>H]-thymidine incorporation. Finally, the medium was removed and the cells were detached with 100 µL/well of 0.25 % trypsin-EDTA solution (Life Technologies, Zug, Switzerland) at 37°C. After 10 min, cellular DNA was precipitated by the addition of 100 µL/well of 20 % (w/v) ice cold trichloroacetic acid (final concentration 10 %) and incubation on ice for 1 hour. The DNA was collected with the cell harvester on glass fiber filters (Unifilter-96, GF/C) (Perkin Elmer, Schwerzenbach,

Switzerland). The filters were dried, liquid scintillator (Microscint 20) (Perkin Elmer, Schwerzenbach, Switzerland) was added and the plate was subjected to liquid-scintillation counting (TopCount) (PerkinElmer, Schwerzenbach, Switzerland).

**[<sup>3</sup>H]-proline incorporation assays.** With this assay extracellular matrix synthesis (collagens and fibonectin contain high amounts of proline) as a measure of fibrosis is determined. Human PASMNC were seeded at a density of 10,000 cells/well onto fibronectin-coated 96-well plates in 100  $\mu$ l/well complete growth medium and cultured for 8 - 15 h at 37°C / 5 % CO<sub>2</sub>. Then medium was exchanged for 100  $\mu$ L/well starvation medium and after overnight incubation, cells were supplemented with a dilution series (10  $\mu$ L/well) of ACT-333679 or iloprost and with 25 or 50 ng/mL human recombinant PDGF-BB (Sigma Aldrich, Buchs, Switzerland) or of vehicle. Cells were cultivated at 37°C / 5 % CO<sub>2</sub> for 40 h. During the last 24 hours of this incubation period, the wells were supplemented with 10  $\mu$ L/well of L-[2,3-<sup>3</sup>H]-proline in starvation medium (0.2  $\mu$ Ci/well) (Perkin Elmer, Schwerzenbach, Switzerland). For determination of [<sup>3</sup>H]-proline incorporation, cell supernatants were discarded, cells were lysed in 150  $\mu$ L/well NaOH (0.15 M) and lysates were incubated on ice for 30 min. For protein precipitation, 100  $\mu$ L/well of trichloroacetic acid (50% (w/v) stock, final concentration=20%) was added and the lysates were incubated on ice for 30 min. Precipitated proteins were collected with the Filtermate cell harvester (Perkin Elmer, Schwerzenbach, Switzerland) onto glass fiber filters (Unifilter-96, GF/C) (Perkin Elmer, Schwerzenbach, Switzerland), filters were washed 8x with deionized water, dried and then supplemented with 60  $\mu$ L/well of liquid scintillator (Microscint20) (Perkin Elmer, Schwerzenbach, Switzerland). Then plates were subjected to liquid scintillation counting (TopCount) (Perkin Elmer, Schwerzenbach, Switzerland).

**Cyclic AMP assay.** T-REx- HEK-hIP were seeded at 20,000 cells/well into 96-well plates, and grown overnight in presence of 1 ng/ml or 10 ng/ml tetracycline (Sigma Aldrich, Buchs, Switzerland) to induce low or high IP receptor expression levels, respectively. Cells were washed with assay buffer (1x HBSS: 20 mM Hepes, 0.0375 % NaHCO<sub>3</sub>, 0.1 % fatty acid free BSA) and then subjected to agonist dilution series in assay buffer in the presence of 3-isobutyl-1-methylxanthine (IBMX, 0.5 mM) (Sigma Aldrich, Buchs, Switzerland). After 30 min, cells were lysed, cAMP levels were determined using the Tropic cAMP-screen System (ThermoFisher Scientific, Reinach, Switzerland) and luminescence was read with a Synergy4 microplate reader (BioTek Instruments, Winooski, VT, USA). Data were converted into concentration-response curves and EC<sub>50</sub> values and E<sub>max</sub> values were calculated with the proprietary IC<sub>50</sub> witch software (Actelion Pharmaceuticals Ltd., Allschwil, Switzerland), using the compound intrinsic maximum and minimum as plateau values. Compound E<sub>max</sub> values were compared to the maximal efficacy of iloprost (100 %). For PASMC, a slightly modified protocol was used: 10,000 cells/well were seeded and cultivated for 48 hours in differentiation medium, and 6 hours in starvation medium before stimulation with IP receptor agonists for 30 min.

**β-arrestin recruitment assay.** CHO-hIP PathHunter® cells were detached, seeded in 384-well plates and grown overnight in OptiMEM medium (Life Technologies, Zug, Switzerland) containing 1 % FBS heat-inactivated. Compounds were incubated with cells for 90 min at 37°C. After addition of the FLASH detection reagent (Discoverx, Birmingham, UK), luminescence was read using a fluorescence imaging plate reader (FLIPR Tetra) (Molecular Devices, Sunnyvale, CA, USA). The maximum signal per well was exported to generate concentration-response curves and EC<sub>50</sub> and E<sub>max</sub> values were calculated with the proprietary IC<sub>50</sub> witch software, using the compound intrinsic curve maximum and minimum as plateau values. Compound efficacies were compared to the maximal efficacy of iloprost (100 %).

**Internalization assay by immunofluorescence microscopy.** CHO-hIP cells were seeded into 8-chamber slides (BD Falcon, Allschwil, Switzerland) and grown overnight. IP receptor agonists were added and incubated for 20 h. Cells were fixed in 3 % paraformaldehyde (Sigma Aldrich, Buchs, Switzerland), permeabilized and stained in phosphate buffered saline (PBS), 10 % FBS heat-inactivated, 0.1 % saponin (Sigma Aldrich, Buchs, Switzerland), using mouse anti-hIP receptor antibodies 13-Q (1 µg/ml; Cat.No.sc-100308, Santa Cruz Biotechnology Inc., Dallas, TX, USA) and Alexa Fluor 488 goat anti-mouse antibodies (Life Technologies, Zug, Switzerland). Nuclei were stained with Hoechst 33342 (Life Technologies, Zug, Switzerland).

### **Analysis of IP receptor internalization by flow cytometry**

Isogenic T-REx-HEK-hIP cells were seeded into 12-well plates and IP receptor was induced by cultivation in 10 ng/ml tetracycline for 24 h, to induce IP receptor expression levels sufficiently high for flow cytometric detection. Agonist dilution series were then added in low serum medium (0.5% FBS). After incubation with agonists for indicated times, the cells were washed with PBS and detached by rapid trypsinization and quenching with trypsin inhibitor. Then, IP receptors were stained with mouse anti-Flag antibodies (1:1000; Cat.No.F-3165, Sigma, St.Louis, MO, USA), diluted in PBS / 2 mM EDTA and 0.5 % fatty acid free BSA (Calbiochem, San Diego, CA, USA). As secondary antibody Alexa Fluor 488 goat anti-mouse IgG (Life Technologies, Zug, Switzerland) was used. Then, propidium iodide-negative cells were analyzed using the flow cytometer FACS Aria IIu (BD Biosciences, Heidelberg, Germany). Median fluorescence intensity of every sample was corrected for the background fluorescence of parental cells not expressing the IP receptor and was then used to quantify cellular IP receptor expression levels.

**In vivo studies.** Male Wistar and spontaneously hypertensive rats (SHR) were obtained from Harlan Laboratories Ltd. (Horst, The Netherlands). All rats were maintained under identical conditions in climate-controlled conditions (18 to 22 °C, 40% to 60% relative

humidity), with a 12:12-hour light:dark cycle in accordance with the guidelines of the Baselland Cantonal Veterinary Office.

SHRs were pretreated with buprenorphine (Temgesic®, 0.03 mg/kg, Essex Chemie AG, Lucerne, Switzerland) and anesthesia was induced and maintained by inhalation of 2 - 4 % isoflurane (100 % O<sub>2</sub>). The abdomen was then opened with a midline abdominal laparotomy, and a blood pressure sensing catheter was placed in the descending aorta below the renal arteries, pointing upstream. The blood-pressure transmitter (TA11PA C40, Data Sciences International, New Brighton, MN, USA) was implanted into the peritoneal cavity under sterile conditions. The transmitter was sutured to the inside of the abdominal wall. Following surgery, rats were transferred into a dedicated recovery room, and monitored for 3-4 days. Buprenorphine (0.03 mg/kg subcutaneous (s.c.) injection) was administered once daily for 2 days after surgery. A similar methodology was used for transmitter implantation in MCT-PH rats.

The blood-pressure transmitter was placed in the abdominal cavity, and the sensing catheter was positioned in the thorax by using a trocar. After removal of the trocar, the right ventricle was punctured and the sensing catheter inserted into the right ventricle and pushed into the pulmonary artery. Rats were monitored for 4 days after surgery with administration of buprenorphine (0.03 mg/kg s.c.) once daily. Three weeks after the implantation of telemetry devices, rats were treated with MCT (Sigma Chemicals, St.Louis, MO, USA) as a single s.c. injection (60 mg/kg). Four to five weeks after injection of MCT, rats became pulmonary hypertensive and the effects of repeated oral administration of selexipag on pulmonary arterial pressure were evaluated.

Telemetry units were obtained from Data Sciences (New Brighton, MN, USA). The implanted sensor consisted of a fluid-filled catheter (0.7 mm diameter, 8 or 10 cm long; model TA11PA C40) connected to a highly stable low-conductance strain-gauge pressure transducer, which measures the absolute arterial pressure relative to vacuum, and of a radio-frequency

transmitter. Gas sterilized and pre-calibrated implants were provided by the manufacturer. Before implantation of the transmitters, calibration was verified to be accurate within 5 mmHg. The transmitter signals were coded and monitored by a receiver (RPC-1, Data Sciences). The signal from the receiver was consolidated by a multiplexer (Data Exchange Matrix, Data Sciences) and sent to a designated personal computer (Dell, Optiplex, 960). Arterial pressures were normalized by using input from an ambient-pressure reference (APR-1, Data Sciences, New Brighton, MN, USA).

Systemic or pulmonary arterial pressures were collected at 5 min intervals throughout the experimental period using the Dataquest ART Gold acquisition system (version 4.3). Blood pressure signals were sampled at 500 Hz. 5 min intervals or hourly means of mean systemic arterial pressure (MAP) or mean pulmonary arterial pressure (MPAP) were calculated. The 24 hour period before treatment was used as the control period and each rat served as its own control by using the data from the 24 hours before treatment. HR was derived from the pressure waveform.

Osmotic infusion pumps (ALZET®, 2ML1 and 2ML2 models, Cupertino, CA, USA) were used to deliver selexipag and treprostinil as continuous intravenous infusions. In brief, rats were pretreated with buprenorphine (0.03 mg/kg, s.c.) and anesthetized with 2-4% isoflurane (100 % O<sub>2</sub>). The jugular vein was cannulated and the pump was implanted under the skin mid-scapula. The wound was closed using medical tissue adhesive and disposable skin staple.

All *in vivo* results are presented as mean  $\pm$  SEM. Maximal effects between MAP and MPAP vs. control period are expressed in mmHg.

**Determination of ACT-333679 (active metabolite of selexipag) and treprostinil plasma concentrations.** Selexipag is the parent drug of the active metabolite ACT-333679 (Kuwano et al., 2007). After i.v. administration of selexipag or treprostinil, blood samples (250  $\mu$ L) were collected in 5 % EDTA (K2E EDTA, BD Microtainer Ref 365975) and centrifuged at

10,000 g / 4 °C. The plasma samples were put in a 96-well PCR plate and stored at -20 °C. Plasma samples were analyzed for ACT-333679 or treprostinil concentrations using liquid chromatography coupled to tandem mass spectrometry (LC-MS/MS) and a deuterated internal standard for ACT-333679. The analytical equipment consisted of a Shimadzu HPLC System (Shimadzu, Reinach, Switzerland) connected to an API5000 (AB SCIEX, Concord, ON, Canada). Data acquisition was performed with the Analyst software package. The chromatographic analysis was achieved on a Phenomenex RP Polar column (4 µm, 2.0 x 20 mm ID) for ACT-333679 or on a Phenomenex Luna C8 column (5 µm, 2.0 x 20 mm ID) for treprostinil, at room temperature with a flow rate of 0.6 ml/min (Phenomenex, Torrance, CA). Mobile phases consisted of 0.1% aqueous formic acid (ACT-333679) or ammonium formate 5 mM pH 9 (treprostinil) and acetonitrile. The mass transitions used for ACT-333679, its deuterated standard and treprostinil were, 420.4 to 378.3 and 427.4 to 379.4 and 389.1 to 331.5, respectively, all with a scan time of 50 milliseconds. The inclusion of quality control samples with acceptance criteria of  $\pm 15\%$  in the bioanalytical runs was used to check the performance of the assays.

## RESULTS

### **ACT-333679 is an efficacious and potent inhibitor of PASMCM contraction, proliferation and extracellular matrix production.**

ACT-333679 was compared in terms of potency and efficacy with the prototypic PGI<sub>2</sub> analog iloprost, using human primary PASMCM. In those cells we measured a set of PAH-relevant phenotypic parameters, including cytoskeletal contraction, cell proliferation and extracellular matrix (ECM) production. PASMCM relaxation is mediated by the cAMP-dependent phosphorylation of myosin light chain kinase (MLCK), which leads to a decrease in kinase affinity for Ca<sup>2+</sup> / calmodulin and reduced enzymatic activity. This results in lower myosin light chain phosphorylation and activation (Horman 2008). We therefore investigated if the IP receptor agonists ACT-333679 or iloprost increased MLCK phosphorylation in PASMCM. Both ACT-333679 and iloprost resulted in a concentration-dependent increase in MLCK phosphorylation with comparable maximal efficacies and EC<sub>50</sub> values of ~3 nM and ~0.1 nM, respectively (Figure 2A, B). Equal maximal efficacies in PAH-related readouts are important and indicate comparable therapeutic potential. Different potency values, on the other hand are not relevant if the required *in vivo* exposures are reached.

We next analyzed whether the observed effects on MLCK phosphorylation translated to cellular shape changes using the label-free impedance technology (Nayler et al., 2010). Both compounds induced a concentration-dependent, rapid and pronounced decrease in impedance (shown for ACT-333679 in Figure 2C) indicating cytoskeletal relaxation. Minimum impedance values within the first 3 hours after stimulation were used to generate concentration response curves (Figure 1D). ACT-333679 and iloprost had equal maximal efficacies and displayed respective EC<sub>50</sub> values of 4.3 nM (n=3;  $\sigma_g$  =1.2) and 0.12 nM (n=3;  $\sigma_g$ =1.1), i.e. the potency values were very comparable to those seen in the MLCK-P assay. The parent compound of ACT-333679, selexipag, had an EC<sub>50</sub> value of 157 nM (n=3,

$\sigma_g=1.3$ ), i.e. 37-fold less potent than its active metabolite, and had a maximal efficacy comparable to that of the other two agonists. The myosin inhibitor blebbistatin decreased PASMC impedance in a concentration-dependent manner to a comparable extent and with similar onset of action and kinetics as ACT-333679, suggesting that PASMC shape changes that are induced by IP receptor agonist stimulation reflect actomyosin relaxation (Figure 2E).

Next we analyzed whether ACT-333679 could also counteract ET-1-induced PASMC contraction. PASMC were pre-stimulated with 10 nM ET-1 and after reaching a response plateau, IP receptor agonists were added (shown for ACT-333679 in Figure 2F). ACT-333679 or iloprost induced a concentration-dependent decrease of impedance with comparable maximal efficacies for both agonists and a mean potency for ACT-333679 of  $IC_{50}=13$  nM ( $n=2$ ), and for iloprost of  $IC_{50}=2.3$  nM ( $n=2$ ). Concentration-response curves were generated from impedance data at the 190 min time point (Figure 2G). To visualize this cellular shape change, PASMC were monitored in real time using a tomographic microscope. ET-1 (100 nM) addition induced strong contraction of PASMC within less than 30 min. Addition of ACT-333679 (1  $\mu$ M) after 70 min reverted this contraction (Figure 3A). In contrast, addition of vehicle instead of ACT-333679 did not revert the ET-1 induced contraction (Figure 3B) nor did it induce cellular shape change at either time points (Figure 3C). The corresponding movies can be viewed under <http://orbit.actelion.com/selexipag/>. These data suggest that IP receptor agonists effectively attenuated pro-contractile signaling pathways and actomyosin contraction in PASMC.

The potential anti-proliferative activity of ACT-333679 and iloprost was also investigated. PDGF-BB, which has been proposed to contribute to the development of PAH, induces proliferation and extracellular matrix production of vascular smooth muscle cells. PDGF-BB decreases the expression of p27(Kip1), an inhibitor of cyclin dependent kinases, and increases expression of cyclin D<sub>1</sub> (Weber et al., 1997). A 24 hour PDGF-BB treatment of quiescent PASMC strongly decreased p27(Kip1) expression which was concentration-

dependently and potently attenuated by co-treatment with ACT-333679 and iloprost (Figure 4A). Also, PDGF-BB treatment of PASMC strongly induced cyclin D1 expression which was again concentration-dependently and potently reduced by ACT-333679 or iloprost co-treatment (Figure 4B). Furthermore, to quantify PDGF-BB-induced PASMC proliferation, [<sup>3</sup>H]-thymidine incorporation was used. The normalized data of at least 10 experiments per compound were pooled and average values (+/-SEM) are presented. Both ACT-333679 and iloprost partially reduced PDGF-BB-induced PASMC proliferation with similar maximal efficacies (~20%) and with IC<sub>50</sub> values of 4.0 nM and 0.11 nM, respectively (Figure 4C). Finally, we analyzed the effects on PDGF-BB-induced cellular [<sup>3</sup>H]-proline incorporation, as a measure of extracellular matrix protein neo-synthesis. Both ACT-333679 and iloprost partially reduced ECM synthesis with similar maximal efficacies (~40%) and with IC<sub>50</sub> values of 8.3 nM (n=3) and 0.68 nM (n=3) (Figure 4D, normalized data +/- SEM).

Thus, the non-prostanoid selective IP receptor agonist, ACT-333679, displayed efficacy in all tested PAH-related phenotypic parameters in PASMC comparable to that of the prototypic PGI<sub>2</sub> analog iloprost, and with a 10- to 30-fold lower potency.

### **ACT-333679 is a partial agonist in receptor-proximal cAMP accumulation assays.**

After having analyzed two IP receptor agonists in receptor-distal, PAH-relevant phenotypic assays, we investigated the activation of IP receptor-proximal intracellular signaling pathways in PASMC. To that end, we analyzed the cAMP increase in PASMC in response to selexipag, ACT-333679, iloprost and the additional PGI<sub>2</sub> analogs beraprost and treprostinil.

All IP receptor agonists induced cAMP synthesis in a concentration-dependent and saturable manner (except the parent drug selexipag, which did not reach an efficacy plateau) (Figure 5A). Interestingly, ACT-333679 behaved as partial agonist with a maximal efficacy of 56% when compared to the three PGI<sub>2</sub> analogs, all of which had similar maximal efficacies of

~100%. Intrinsic compound potencies ranged from 16 nM (iloprost) to 214 nM (ACT-333679) (Table 1). Thus, in receptor-proximal cAMP synthesis partial agonism of ACT-333679 was uncovered, a property not seen when measuring receptor-distal phenotypic parameters in PASMC. In addition, due to its receptor-proximal position in the signaling cascade, potency of the agonists in the cAMP readout was ~50-100-fold lower than in receptor-distal assays.

Appearance of partial agonism not only depends on the position of a readout in the signaling cascade, but also on the cellular receptor reserve, i.e. cellular receptor expression levels. We thus characterized the different IP receptor agonists in cells with high and low receptor expression levels using a tetracycline-inducible T-REx-HEK-hIP cell line. Cell treatment with the lowest (0.1 ng/ml) and the highest (10 ng/ml) concentration of tetracycline resulted in a 60-fold difference in receptor expression as analyzed by immunoblotting (Figure 5B). Parental cells did not show a cAMP response (Figure 5C, left panel). In HEK-high hIP cells, all compounds behaved as full agonists (Figure 5C middle panel, Table 1) with a potency of 0.53 nM for iloprost, 29 nM for ACT-333679 and 813 nM for selexipag. In contrast, in HEK-low hIP cells (Figure 5C, right panel, Table 1) the non-prostanoid agonists displayed partial agonism ( $E_{\max}$ =45% for ACT-333679, selexipag did not reach saturation), whereas the PGI<sub>2</sub> analogs were full agonists. Furthermore, in HEK-low hIP cells all five agonists displayed potencies that were comparable to those observed in PASMC (Figure 5A and Table 1). We conclude that ACT-333679 (and likely also selexipag) is a partial agonist at the recombinant and naturally expressed IP receptor, and this property is only uncovered in cell systems with low receptor expression using a receptor-proximal readout. Previous cAMP measurements in recombinant cells expressing the IP receptor had not detected this partial agonism most likely due to higher IP receptor expression levels (Kuwano et al., 2007). In addition, selexipag is 28-fold less potent than the active metabolite ACT-333679 (cAMP assays in HEK-high IP), comparable to the factor observed in the PASMC impedance assays (37-fold). This shows that in both recombinant and primary cells, the metabolite ACT-333679 is much more potent

than selexipag which explains why ACT-333679 is regarded as the main contributor to pharmacological effects in vivo.

### **ACT-333679 has low $\beta$ -arrestin recruitment and IP receptor internalization activity.**

Lack of receptor internalization / desensitization is a favorable property for chronically dosed IP receptor agonists. GPCR agonists with partial agonism in second messenger measurements have previously been shown to display partial agonism in other receptor-proximal molecular events such as  $\beta$ -arrestin recruitment and receptor internalization (Clark et al., 1999), i.e. processes that usually render cells insensitive to further stimulation. To investigate this aspect, ACT-333679, selexipag and the PGI<sub>2</sub> analogs beraprost, treprostinil and iloprost were characterized in  $\beta$ -arrestin recruitment assays. The PGI<sub>2</sub> analogs behaved as high efficacy agonists (iloprost, beraprost,  $E_{\max}$ =90-100%, treprostinil;  $E_{\max}$ =67%). In contrast, the non-prostanoid agonists ACT-333679 ( $E_{\max}$ =40%) and selexipag ( $E_{\max}$ =24%) displayed significantly reduced maximal  $\beta$ -arrestin recruitment efficacy. The intrinsic potencies of iloprost and ACT-333679 were similar, with EC<sub>50</sub> values of 35 nM and 51 nM, respectively. Treprostinil and beraprost showed EC<sub>50</sub> values of ~200 nM. Selexipag displayed low potency with EC<sub>50</sub> around 800 nM (Figure 6, Table 2).

To determine whether the differences in  $\beta$ -arrestin recruitment efficiency caused different degrees of receptor internalization, CHO-hIP cells were treated with IP receptor agonists and IP receptor localization was analyzed by immunofluorescence microscopy. All cells displayed a moderate degree of constitutive receptor internalization even in absence of agonist treatment (vehicle, Figure 7). However, treatment with the PGI<sub>2</sub> analogs induced a strong perinuclear accumulation of receptors and depletion from the cell surface. This internalization was concentration-dependent. Detectable internalization was observed for iloprost starting at 100 nM and for beraprost and treprostinil at 1  $\mu$ M, which is in good agreement with the

efficient  $\beta$ -arrestin recruitment observed at these concentrations (Figure 7). In contrast, the non-prostanoid agonists ACT-333679 and selexipag did not induce detectable intracellular IP receptor accumulation, even at the highest tested concentration of 10  $\mu$ M and did not quantitatively deplete IP receptors from the plasma membrane. These findings were confirmed by flow cytometric quantification of cell surface receptor expression in cells treated with the various agonists (Figure 8) where the PGI<sub>2</sub> analogs induced concentration- and time-dependent reduction of surface receptor expression while ACT-333679 did not. In fact, ACT-333679 increased the IP receptor surface expression, a phenomenon known for non-internalizing GPCR ligands, mostly antagonists (Wueller et al., 2004).

Thus, in summary, while displaying full efficacy on PAH-related phenotypic parameters, the selexipag metabolite, ACT-333679, has a low  $\beta$ -arrestin recruitment and receptor internalization activity.

### **Selexipag does not cause tachyphylaxis in vivo.**

The effects of repeated oral administration of selexipag on MPAP were determined in the rat monocrotaline model of PH (Figure 9). The effects of bi-daily oral administration of a sub-maximal dose of selexipag (10 mg/kg) were measured over five days. Selexipag decreased MPAP after each administration for ~2 hours. Maximal decreases in MPAP were  $21 \pm 6$  mmHg (morning administration) and  $21 \pm 3$  mmHg (evening administration) when compared to the 1 hour control period. There was no significant difference between the effect of selexipag on MPAP following morning and evening administration throughout the duration of the experiment ( $p > 0.05$ ).

Since the time interval (approximately 12 hours) between bi-daily oral administration of selexipag may have been sufficient to allow for IP receptor resensitization, the effects of continuous i.v. infusion of selexipag were determined in conscious SHR by measuring MAP. The hemodynamic effect of selexipag (1 mg/kg/hour) was sustained for the whole

experimental period of 7 days (maximum decrease in MAP  $25 \pm 5$  mmHg), and MAP values returned to pre-drug levels after cessation of treatment and no re-bound effect was observed (Figure 10A). In the same model the hemodynamic effects of selexipag were compared against treprostinil (Figure 10B and C). Continuous infusion of selexipag (1 mg/kg/hour) decreased MAP maximally by  $21 \pm 8$  mmHg over the observed 48 hours with no development of tachyphylaxis. The plasma concentrations of ACT-333679 are shown in Table 3. In comparison, treprostinil (30  $\mu$ g/kg/hour i.v.) decreased MAP maximally by  $30 \pm 3$  mmHg. The maximal hemodynamic effect of treprostinil was similar to that of selexipag, however, MAP levels returned to pre-drug levels within 36 hours despite continuous infusion and continued presence of treprostinil in plasma (Table 4).

## DISCUSSION

IP receptor agonists elevate intracellular cAMP levels and inhibit contraction and proliferation of PASMC. However, agonists of G protein-coupled receptors can also trigger receptor internalization/desensitization leading to loss in efficacy or a need for higher agonist concentrations. Indeed, PGI<sub>2</sub> analogs such as cicaprost and iloprost induce IP receptor internalization (Smyth et al., 2000; Keefe et al., 2008). Consistent with such in vitro findings, it has been proposed that the clinical efficacy of PGI<sub>2</sub> and its analogs might diminish over time, a phenomenon termed tachyphylaxis, requiring that the dose be increased to maintain efficacy (Rubin et al., 1990; Archer et al., 1996; Shapiro et al., 1997; Barst et al., 2003). Time-dependent loss of vasodilator efficacy of iloprost in perfused rabbit lungs supports these clinical findings (Schermuly et al., 2007).

Analysis of the receptor activation and desensitization profile of ACT-333679 revealed a potent and fully efficacious activation of the receptor-distal events of the cAMP pathway; namely PASMC relaxation, anti-proliferation and anti-fibrosis. However, markedly reduced maximal efficacy in the receptor-proximal events such as cAMP accumulation,  $\beta$ -arrestin recruitment and IP receptor internalization was observed (Figure 11). In contrast, the PGI<sub>2</sub> analogs beraprost, treprostinil and iloprost were full agonists showing maximal efficacy on receptor-proximal assays. Consistent with the limited in vitro desensitization potential, selexipag induced sustained vasodilation in two rat disease models, while the PGI<sub>2</sub> analog treprostinil displayed tachyphylaxis, i.e. loss of effect upon continued administration.

Efficacy/potency differences in G protein signaling versus desensitization have previously been observed for AT<sub>1</sub> agonists, S1P<sub>1</sub> agonists, opioid receptor agonists and GPR109A agonists (Zhou et al., 2013; Schmidt et al., 2013; Raehal and Bohn, 2014; Gatfield et al., 2014; Rajagopal et al., 2006; Violin et al., 2010; Walters et al., 2009; Semple et al., 2008). Several mechanisms can explain such so-called biased GPCR agonism. First, an agonist might stabilize only a subset of receptor conformations, which then leads to preferential activation of a subset of downstream pathways. Second, differential agonist resistance to

intracellular degradation can lead to a bias in the apparent GPCR activation/desensitization ratio (Gatfield et al., 2014). Thirdly, biased behavior can be displayed by partial GPCR agonists having limited efficacy in receptor-proximal readouts such as  $\beta$ -arrestin recruitment and internalization, but full efficacy on receptor-distal phenotypic parameters.

The biased behaviour of ACT-333679 is explained by the third mechanism. ACT-333679 as partial agonist displays submaximal ability to convert its target receptor into the active state even at full occupancy. This is reflected in the partial activation of receptor-proximal processes such as cAMP accumulation,  $\beta$ -arrestin recruitment and receptor internalization. However, the partial activation of receptor-proximal signaling does not limit efficacy in therapeutically relevant receptor-distal phenotypic readouts due to signal amplification along the signaling cascade (Figure 11). This is exemplified by the equal maximal efficacies of ACT-333679 and iloprost in all tested receptor-distal readouts in PASMC such as anti-contraction (modulation of MLCK phosphorylation, shape change) and anti-remodeling (modulation of cyclinD1 and p27 expression, [ $^3$ H]-thymidine and [ $^3$ H]-proline incorporation). While lower maximal efficacy on such parameters would translate to lower in vivo activity, a difference in agonist potency (iloprost being 10- to 30-fold more potent than ACT-333679) does not represent a major hurdle because lower potency can be compensated by higher exposure. Signal amplification along the cAMP-PKA cascade has previously been reported for platelets in which slight increases in cytosolic cAMP levels by treatment with phosphodiesterase inhibitors already lead to a strong increases in PKA activity and inhibition of platelet aggregation (Seiler, 1987). Partial GPCR agonism causing lack of desensitization/internalization has been previously described for other GPCR – agonist systems such as the  $\beta$ 2 adrenergic receptor, the M3 muscarinic receptor or the chemokine receptor 5 (CCR5) (Clark et al., 1999; January et al., 1997; Szekeres et al., 1998; Oppermann et al., 1999). These studies and ours suggest that partial agonism allows to circumvent receptor desensitization while still retaining efficacy in receptor-distal therapeutically relevant readouts.

Based on these in vitro results, we analyzed the IP receptor activation and tachyphylaxis potential of selexipag in different rat models of hypertension. Continuous administration of selexipag caused reduction in MPAP and MAP in rat models of pulmonary or systemic hypertension respectively, with no evidence of tachyphylaxis in either model. Even upon continuous infusion - the most stringent method to assess desensitization in vivo - selexipag reduced MAP in SHR without any signs of tachyphylaxis. In contrast, continuous i.v. infusion of the PGI<sub>2</sub> analog treprostinil induced tachyphylaxis within 36 hours in SHRs despite the continued presence of the drug in plasma.

Additional mechanisms not related to differential  $\beta$ -arrestin recruitment may contribute to the lack of tachyphylaxis seen for selexipag. For example, the high selectivity of selexipag and ACT-333679 for the IP receptor over other prostanoid receptors (Kuwano et al., 2007; Gatfield et al., 2016) might contribute to the absence of tachyphylaxis. Indeed, continuous infusion of the non-selective PGI<sub>2</sub> analog iloprost elicited vasodilatation of perfused rabbit lungs that decreased over time (Schermyly et al., 2007). Iloprost can activate calcium-coupled contractile EP<sub>1</sub> receptors (Abramovitz et al., 2000), and tachyphylaxis was partially prevented by inclusion of an EP<sub>1</sub> receptor antagonist in the perfusate (Schermyly et al., 2007). These data suggest that a pharmacological interaction between IP and EP<sub>1</sub> receptor subtypes contributes to the loss of efficacy to iloprost in this model. It can therefore be postulated that tachyphylaxis is lower for *selective* IP receptor agonists, an additional mechanism potentially contributing to the sustained efficacy of selexipag in vivo.

Taken together, the non-prostanoid agonists selexipag and ACT-333679 not only differ structurally from PGI<sub>2</sub> analogs, but also differ in their molecular pharmacological effects. In the present study we show that ACT-333679 displays full anti-contractile and anti-remodeling efficacy comparable to that of iloprost in PASMC, but a very limited capacity for  $\beta$ -arrestin recruitment and IP receptor internalization in contrast to all tested PGI<sub>2</sub> analogs. This biased efficacy/desensitization ratio of ACT-333679 might contribute to the sustained efficacy of

selexipag observed in animal models and humans (Sitbon et al., 2015).

## **ACKNOWLEDGEMENTS**

The authors thank Julia Friedrich and Stephanie Hertzog for the bioanalytical evaluation of rat plasma samples. We thank Rolf Studer for the design/cloning of the IP receptor expression constructs. We thank Manuel Stritt for the conversion of the time lapse image sequence into a movie.

## **AUTHORSHIP CONTRIBUTIONS**

Participated in research design: J.G., K.Me., D.W., C.G., L.M., K.Mo., P.H.

Conducted experiments: J.G., K.Me., D.W., L.M.

Performed data analysis: J.G., K.Me., D.W., C.G., L.M., K.Mo., P.H.

Wrote or contributed to the writing of the manuscript: J.G., K.Me., D.W., C.G., K.Mo., M.I.,  
M.C., O.N.

## REFERENCES

- Abramovitz M, Adam M, Boie Y, Carrière MC, Denis D, Godbout C, Lamontagne S, Rochette C, Sawyer N, Tremblay NM, Belley M, Gallant M, Dufresne C, Gareau Y, Ruel R, Juteau H, Labelle M, Ouimet N, and Metters KM (2000) The utilization of recombinant prostanoid receptors to determine the affinities and selectivities of prostaglandins and related analogs. *Biochimica et Biophysica Acta* **1483**: 285-293.
- Archer SL, Mike D, Crow J, Long W and Weir EK (1996) A placebo-controlled trial of prostacyclin in acute respiratory failure in COPD. *Chest* **109**:750-755.
- Arehart E, Stitham J, Asselbergs FW, Douville K, MacKenzie T, Fetalvero KM, Gleim S, Kasza Z, Rao Y, Martel L, Segel S, Robb J, Kaplan A, Simons M, Powell RJ, Moore JH, Rimm EB, Martin KA, Hwa J (2008) Acceleration of cardiovascular disease by a dysfunctional prostacyclin receptor mutation: potential implications for cyclooxygenase-2 inhibition. *Circ Res* **102**:986-993.
- Asaki T, Kuwano K, Morrison K, Gatfield J, Hamamoto T, Clozel M (2015) Selexipag: An Oral and Selective IP Prostacyclin Receptor Agonist for the Treatment of Pulmonary Arterial Hypertension. *J Med Chem* **58**:7128-7137
- Barst RJ, Rubin LJ, Long WA, McGoon MD, Rich S, Badesch DB, Groves BM, Tapson VF, Bourge RC, Brundage BH, Koerner SK, Langleben D, Keller CA, Murali S, Uretsky BF, Clayton LM, Jöbsis MM, Blackburn SD, Shortino D, Crow JW; Primary Pulmonary Hypertension Study Group (1996) A comparison of continuous intravenous epoprostenol (prostacyclin) with conventional therapy for primary pulmonary hypertension. *N Engl J Med* **334**:296-301.
- Barst RJ, McGoon M, McLaughlin V, Tapson V, Rich S, Rubin L, Wasserman K, Oudiz R, Shapiro S, Robbins IM, Channick R, Badesch D, Rayburn BK, Flinchbaugh R, Sigman J, Arneson C, Jeffs R; Beraprost Study Group (2003) Beraprost therapy for pulmonary arterial hypertension. *J Am Coll Cardiol* **41**: 2119-2125.

Beamish JA, He P, Kottke-Marchant K, Marchant RE (2010) Molecular regulation of contractile smooth muscle cell phenotype: implications for vascular tissue engineering. *Tissue Eng Part B Rev*. **16**:467-91

Boie Y, Rushmore TH, Darmon-Goodwin A, Grygorczyk R, Slipetz DM, Metters KM, Abramovitz M (1994) Cloning and expression of a cDNA for the human prostanoid IP receptor. *J Biol Chem* **269**:12173-12178

Christman BW, McPherson CD, Newman JH, King GA, Bernard GR, Groves BM, Loyd JE (1992) An imbalance between the excretion of thromboxane and prostacyclin metabolites in pulmonary hypertension. *N Engl J Med* **327**:70-75.

Clark RB, Knoll BJ, Barber R (1999) Partial agonists and G protein-coupled receptor desensitization. *Trends Pharmacol Sci* **20**:279-286.

Galiè N, Hoeper MM, Humbert M, Torbicki A, Vachiery JL, Barbera JA, Beghetti M, Corris P, Gaine S, Gibbs JS, Gomez-Sanchez MA, Jondeau G, Klepetko W, Opitz C, Peacock A, Rubin L, Zellweger M, Simonneau G; ESC Committee for Practice Guidelines (CPG) (2009) Guidelines for the diagnosis and treatment of pulmonary hypertension: the Task Force for the Diagnosis and Treatment of Pulmonary Hypertension of the European Society of Cardiology (ESC) and the European Respiratory Society (ERS), endorsed by the International Society of Heart and Lung Transplantation (ISHLT). *Eur Heart J* **30**: 2493-2537.

Gatfield J, Monnier L, Studer R, Bolli MH, Steiner B, Nayler O (2014) Sphingosine-1-phosphate (S1P) displays sustained S1P1 receptor agonism and signaling through S1P lyase-dependent receptor recycling. *Cell Signal* **26**:1576-1588.

Gatfield J, Menyhart K, Tunis M, Studer R, Ferrari G, Nayler O (2016) Selectivity of the selexipag active metabolite ACT-333679 for the IP receptor avoids DP1/EP2-mediated inhibition of natural killer cell responses in vitro. *Am J Respir Crit Care Med* **193**:A2238

Hasse A, Nilius SM, Schrör K, Meyer-Kirchrath J (2003) Long-term-desensitization of prostacyclin receptors is independent of the C-terminal tail. *Biochem Pharmacol* **65**:1991-1995.

January B, Seibold A, Whaley B, Hipkin RW, Lin D, Schonbrunn A, Barber R, Clark RB (1997) Beta2-adrenergic receptor desensitization, internalization, and phosphorylation in response to full and partial agonists. *J Biol Chem* **272**:23871-23879.

Kuwano K, Hashino A, Asaki T, Hamamoto T, Yamada T, Okubo K, Kuwabara K (2007) 2-[4-[(5,6-diphenylpyrazin-2-yl)(isopropyl)amino]butoxy]-N-(methylsulfonyl)acetamide (NS-304), an orally available and long-acting prostacyclin receptor agonist prodrug. *J Pharmacol Exp Ther* **322**:1181--1188.

McLaughlin VV, Genthner DE, Panella MM, Rich S (1998) Reduction in pulmonary vascular resistance with long-term epoprostenol (prostacyclin) therapy in primary pulmonary hypertension. *N Engl J Med* **338**:273-277.

Morrell NW, Adnot S, Archer SL, Dupuis J, Jones PL, MacLean MR, McMurtry IF, Stenmark KR, Thistlethwaite PA, Weissmann N, Yuan JX, Weir EK (2009) Cellular and molecular basis of pulmonary arterial hypertension. *J Am Coll Cardiol* **54**: S20-31.

Nayler O, Birker-Robaczewska M, Gatfield J (2010) Integration of Label-Free Detection Methods in GPCR Drug Discovery, Wiley, Hoboken, NJ.

Olschewski H, Rose F, Schermuly R, Ghofrani HA, Enke B, Olschewski A, Seeger W (2004) Prostacyclin and its analogues in the treatment of pulmonary hypertension. *Pharmacol Ther* **102**: 139-153.

Oppermann M, Mack M, Proudfoot AE, Olbrich H (1999) Differential effects of CC chemokines on CC chemokine receptor 5 (CCR5) phosphorylation and identification of phosphorylation sites on the CCR5 carboxyl terminus. *J Biol Chem* **274**:8875-8885.

Raehal KM, Bohn LM (2014) Beta-arrestins: regulatory role and therapeutic potential in opioid and cannabinoid receptor-mediated analgesia. *Handb Exp Pharmacol* **219**:427-443.

Rajagopal K, Whalen EJ, Violin JD, Stiber JA, Rosenberg PB, Premont RT, Coffman TM, Rockman HA, Lefkowitz RJ (2006) Beta-arrestin2-mediated inotropic effects of the angiotensin II type 1A receptor in isolated cardiac myocytes. *Proc Natl Acad Sci U S A* **103**:16284-16289.

Rubin LJ, Mendoza J, Hood M, McGoon M, Barst R, Williams WB, Diehl JH, Crow J, Long W (1990) Treatment of primary pulmonary hypertension with continuous intravenous prostacyclin (epoprostenol). Results of a randomized trial. *Ann Intern Med*. 112:485-491

Schermuly RT, Pullamsetti SS, Breitenbach SC, Weissmann N, Ghofrani HA, Grimminger F, Nilius SM, Schrör K, Meger-Kirchrath J, Seeger W and Rose F (2007) Iloprost-induced desensitization of the3 prostacyclin receptor in isolated rabbit lungs. *Respir Res* **8**: 4-16

Schmid CL, Streicher JM, Groer CE, Munro TA, Zhou L, Bohn LM (2013) Functional selectivity of 6'-guanidinonaltrindole (6'-GNTI) at  $\kappa$ -opioid receptors in striatal neurons. *J Biol Chem* **288**:22387-22398.

Seiler S, Arnold AJ, Grove RI, Fifer CA, Keely SL Jr, Stanton HC (1987) Effects of anagrelide on platelet cAMP levels, cAMP-dependent protein kinase and thrombin-induced  $\text{Ca}^{++}$  fluxes. *J Pharmacol Exp Ther* 243:767-774.

Semple G, Skinner PJ, Gharbaoui T, Shin YJ, Jung JK, Cherrier MC, Webb PJ, Tamura SY, Boatman PD, Sage CR, Schrader TO, Chen R, Colletti SL, Tata JR, Waters MG, Cheng K, Taggart AK, Cai TQ, Carballo-Jane E, Behan DP, Connolly DT, Richman JG (2008) 3-(1H-tetrazol-5-yl)-1,4,5,6-tetrahydro-cyclopentapyrazole (MK-0354): a partial agonist of the nicotinic acid receptor, G-protein coupled receptor 109a, with antilipolytic but no vasodilatory activity in mice. *J Med Chem* **51**:5101-5108.

Shapiro SM, Oudiz RJ, Cao T, Romano MA, Beckman XJ, Georgiou D, Mandayam S, Ginzton LE and Brundage BH (1997) Primary pulmonary hypertension: improved long-term effects and survival with continuous intravenous epoprostenol infusion. *J Am Coll Cardiol* **30**: 343-349

Sitbon O, Channick R, Chin KM, Frey A, Gaine S, Galiè N, Ghofrani HA, Hoeper MM, Lang IM, Preiss R, Rubin LJ, Di Scala L, Tapson V, Adzerikho I, Liu J, Moiseeva O, Zeng X, Simonneau G, McLaughlin VV; GRIPHON Investigators (2015) Selexipag for the Treatment of Pulmonary Arterial Hypertension. *N Engl J Med* **373**:2522-2533.

Smyth EM, Austin SC, FitzGerald GA (2002) Activation-dependent internalization of the human prostacyclin receptor. *Adv Exp Med Biol* **507**:295-301.

Smyth EM, Austin SC, Reilly MP, FitzGerald GA (2000) Internalization and sequestration of the human prostacyclin receptor. *J Biol Chem* **275**:32037-32045.

Sykes DA, Dowling MR, Charlton SJ (2009) Exploring the mechanism of agonist efficacy: a relationship between efficacy and agonist dissociation rate at the muscarinic M3 receptor. *Mol Pharmacol* **76**:543-551.

Szekeres PG, Koenig JA, Edwardson JM (1998) The relationship between agonist intrinsic activity and the rate of endocytosis of muscarinic receptors in a human neuroblastoma cell line. *Mol Pharmacol* **53**:759-765.

Tuder RM, Cool CD, Yeager M, Taraseviciene-Stewart L, Bull TM, Voelkel NF (2001) The pathobiology of pulmonary hypertension. Endothelium. *Clin Chest Med* **22**:405-418.

Violin JD, DeWire SM, Yamashita D, Rominger DH, Nguyen L, Schiller K, Whalen EJ, Gowen M, Lark MW (2010) Selectively engaging  $\beta$ -arrestins at the angiotensin II type 1 receptor reduces blood pressure and increases cardiac performance. *J Pharmacol Exp Ther* **335**:572-579.

Walters RW, Shukla AK, Kovacs JJ, Violin JD, DeWire SM, Lam CM, Chen JR, Muehlbauer MJ, Whalen EJ, Lefkowitz RJ (2009) Beta-Arrestin1 mediates nicotinic acid-induced flushing, but not its antilipolytic effect, in mice. *J Clin Invest* **119**:1312-1321.

Weber JD, Hu W, Jefcoat SC Jr, Raben DM, Baldassare JJ (1997) Ras-stimulated extracellular signal-related kinase 1 and RhoA activities coordinate platelet-derived growth factor-induced G1 progression through the independent regulation of cyclin D1 and p27. *J Biol Chem* **272**:32966-32971

Whittle BJ, Silverstein AM, Mottola DM, Clapp LH (2012) Binding and activity of the prostacyclin receptor (IP) agonists, treprostinil and iloprost, at human prostanoid receptors: treprostinil is a potent DP1 and EP2 agonist. *Biochem Pharmacol* **84**: 68-75.

Wikström K, Reid HM, Hill M, English KA, O'Keeffe MB, Kimbembe CC, Kinsella BT (2008) Recycling of the human prostacyclin receptor is regulated through a direct interaction with Rab11a GTPase. *Cell Signal* **20**:2332-46.

Wu Y, O'Callaghan DS, Humbert M (2013) An update on medical therapy for pulmonary arterial hypertension. *Curr Hypertens Rep* **15**: 614-622

Wüller S, Wiesner B, Löffler A, Furkert J, Krause G, Hermosilla R, Schaefer M, Schüle R, Rosenthal W, Oksche AJ (2004) Pharmacochaperones post-translationally enhance cell surface expression by increasing conformational stability of wild-type and mutant vasopressin V2 receptors. *Biol Chem* **279**:47254-63.

Zhou L, Lovell KM, Frankowski KJ, Slauson SR, Phillips AM, Streicher JM, Stahl E, Schmid CL, Hodder P, Madoux F, Cameron MD, Prisinzano TE, Aubé J, Bohn LM (2013) Development of functionally selective, small molecule agonists at kappa opioid receptors. *J Biol Chem* **288**:36703-36716.

## **FOOTNOTES**

All authors of this manuscript are employees and shareholders of Actelion Pharmaceuticals Ltd. No external funding was received

Contact for reprint requests: John Gatfield, Actelion Pharmaceuticals Ltd, Gewerbestrasse 16, 4123 Allschwil, Switzerland, e-mail: john.gatfield@actelion.com

## FIGURE LEGENDS

**Figure 1. Chemical structures of selexipag and its active metabolite ACT-333679.** The parent drug selexipag is enzymatically hydrolyzed in vivo to its active metabolite.

**Figure 2. Efficacy and potency of the IP receptor agonists ACT-333679 and iloprost in receptor-distal actomyosin relaxation readouts in human pulmonary arterial smooth muscle cells.** **A)** MLCK phosphorylation 90 min after agonist stimulation with  $\alpha/\beta$ -tubulin staining as loading control. Representative experiment of n=2. **B)** Mean MLCK-P/tubulin ratios (+/- SD) from two experiments normalized via the maximal response to iloprost (=100%). Significant increase versus vehicle: \* p<0.01; one-sided Student's t-test. **C)** Cells were treated with ACT-333679 or iloprost and impedance changes were recorded (raw traces shown for ACT-333679) and **D)** concentration-response curves for ACT-333679 and iloprost were generated from impedance minima within 3 hours after stimulation. Values represent averages of technical duplicates +/- SD. Representative experiment of n=3. **E)** Raw traces for cells treated with increasing concentrations of the myosin inhibitor blebbistatin **F)** Cells were treated with ET-1 (10 nM) and after 2 hours with IP receptor agonists (impedance raw traces shown for ACT-333679) and **G)** concentration-response curves were generated from impedance values one hour after IP receptor agonist addition. Values represent averages of technical duplicates +/- SD. Representative experiment of n=2 experiments.

**Figure 3. Effect of the IP receptor agonist ACT-333679 on cellular shape change in human pulmonary arterial smooth muscle cells as determined by time lapse tomographic microscopy.** Cells were treated with ET-1 (100 nM) to induce cell contraction. After 70-90 min cells were then either treated with **A)** ACT-333679 (1  $\mu$ M) to induce relaxation or with **B)** vehicle. Alternatively, cells were **C)** treated twice with vehicle.

Tomographic images were taken at regular intervals along the whole experimental period (~180 min) and a set of images along the time course is shown with the baseline cell circumference indicated by a dotted line. Bar: 20  $\mu$ m. Representative sequences of one experiment out of n=3 experiments are shown. The corresponding movie sequences can be accessed via <http://orbit.actelion.com/selexipag/>.

**Figure 4. Efficacy and potency of ACT-333679 and iloprost in receptor-distal proliferation and fibrosis-related readouts in human pulmonary arterial smooth muscle cells.** Immunoblotting for **A)** p27(Kip1) and **B)** cyclinD<sub>1</sub> in serum-starved cells treated with PDGF-BB for 24 hours in the presence of IP receptor agonists.  $\alpha/\beta$ -tubulin staining served as loading control. Representative experiments of n=2. **C)** [<sup>3</sup>H]-thymidine incorporation in serum-starved cells treated with PDGF-BB for 24 hours in the presence of IP receptor agonists. Mean inhibition (+/- SEM) from at least 10 experiments. **D)** [<sup>3</sup>H]-proline incorporation in serum-starved cells treated with PDGF-BB for 40 hours in the presence of IP receptor agonists. Mean inhibition (+/- SEM) of 3 experiments.

**Figure 5. Efficacy and potency of IP receptor agonists in cyclic AMP accumulation assays using human pulmonary arterial smooth muscle cells (PASMC) and cells engineered to express high or low IP receptor levels.** **A)** Responses in PASMC after 30 min of agonist stimulation. Values represent averages of technical duplicates +/- SD. Representative experiment of n=3. **B)** Immunoblot for the hIP receptor in T-REx-HEK parental, and T-REx-HEK-hIP cells induced with increasing concentrations of tetracycline. **C)** Responses after 30 min of agonist stimulation in T-REx-HEK-parental, T-REx-HEK-hIP with high (10 ng/ml tetracycline) or low (1 ng/ml tetracycline) IP receptor expression levels. Values represent averages of technical duplicates +/- SD. Representative experiment of n=2.

**Figure 6. Efficacy and potency of IP receptor agonists at inducing  $\beta$ -arrestin recruitment in CHO cells expressing the human IP receptor.** PathHunter® CHO-hIP cells were treated for 90 min with IP receptor agonists, then  $\beta$ -galactosidase substrate was added and chemiluminescence determined. Values represent averages of technical duplicates ( $\pm$  SD). Representative experiment of n=6 experiments.

**Figure 7. Efficacy and potency of IP receptor agonists at internalizing the recombinant human IP receptor.** CHO-hIP cells were incubated for 20 hours with the different IP receptor agonists. Cells were fixed and stained (IP receptor in green, nuclei in blue). Representative experiment of n=2.

**Figure 8. Efficacy and potency of selected IP receptor agonists at internalizing the recombinant human IP receptor (flow cytometry).** HEK-T-REx-Flag-hIP cells were incubated for the indicated times with dilution series of IP receptor agonists, surface IP receptors were stained with anti-Flag antibodies and quantified by flow cytometry. Values represent the averages of two independent experiments  $\pm$  SD.

**Figure 9. Effect of repeated oral administration of selexipag on MPAP over five days in conscious MCT-PH rats.** Selexipag (10 mg/kg) was administered bi-daily (morning and evening) by oral gavage over five days. MPAP was measured using implanted telemetry systems. Data are presented as means  $\pm$  SEM; n = 7-8

**Figure 10. Effects of intravenous administration of selexipag over 7 days (A) and selexipag (B) and treprostinil (C) over 48 hours on MAP in conscious SHR.** Vehicle or test compounds were administered continuously by iv infusion from implanted osmotic mini-pumps. No hemodynamic recording was possible during surgical implantation of the mini-pumps, as shown by a break in data collection (B and C). The 48 hour period prior to

infusion of vehicle or test compounds was used as the control period for each animal. Data are presented as means  $\pm$  SEM; selexipag, n = 9; treprostinil, n = 15.

**Figure 11. Scheme suggesting how the partial agonism of the selexipag metabolite ACT-333679 at the IP receptor allows to circumvent receptor desensitization while still retaining efficacy in receptor-distal anti-PAH related readouts.** Receptor proximal events in the IP receptor signaling cascade such as cAMP accumulation,  $\beta$ -arrestin recruitment and receptor internalization are activated by ACT-333679 with limited efficacy (partial agonism compared to the fully efficacious PGI<sub>2</sub> analogs) while - due to signal amplification - receptor-distal events such as anti-contraction, anti-proliferation and anti-fibrosis are activated by ACT-333679 with full efficacy (full agonism).

## Tables

**Table 1.** Mean EC<sub>50</sub> values and E<sub>max</sub> values for different IP receptor agonists in cAMP accumulation assays determined in human pulmonary arterial smooth muscle cells (PASMC) or T-REx-HEK-high hIP and T-REx-HEK-low hIP cells.

	PASMC <sup>a</sup> - cAMP		HEK-high hIP <sup>b</sup>		HEK-low hIP <sup>b</sup>	
	EC <sub>50</sub>	E <sub>max</sub>	EC <sub>50</sub>	E <sub>max</sub>	EC <sub>50</sub>	E <sub>max</sub>
	[σg]	[SD]				
ACT-333679	214 nM [1.1]	56 % [5 %]	29 nM [26 nM, 33 nM]	97% [95%, 98%]	277 nM [270 nM, 285 nM]	45 % [51%, 39 %]
selexipag	Nd	29 % [6 %]	813 nM [790 nM, 837 nM]	85% [85%, 84%]	nd	nd
beraprost	94 nM [1.1]	104 % [7 %]	8.6 nM [8.4 nM, 8.9 nM]	89% [91%, 86%]	135 nM [119 nM, 153 nM]	93 % [90%, 96%]
iloprost	16 nM [1.1]	100 % [0 %]	0.53 nM [0.42 nM, 0.67 nM]	100% [100%, 100%]	10 nM [7.8 nM, 13 nM]	100 % [100%, 100%]
treprostinil	107 nM [1.1]	107 % [4 %]	11 nM [11 nM, 12 nM]	96% [97%, 95%]	264 nM [200 nM, 348 nM]	108 % [110%, 106%]

<sup>a</sup> For PASMC, EC<sub>50</sub> values were derived using the individual curve-intrinsic maxima and their geomean is shown. σg: geometric standard deviation. E<sub>max</sub>: maximal efficacy compared to that of iloprost; arithmetic mean is shown. SD: arithmetic standard deviation. n=3 measurements.

<sup>b</sup> For HEK cells, EC<sub>50</sub> values were derived using the individual curve-intrinsic maxima. Shown are geometric means with individual values in brackets. E<sub>max</sub>: maximal efficacy compared to that of iloprost. Shown are arithmetic means with individual values in brackets. n=2 measurements.

**Table 2.** Mean EC<sub>50</sub> and E<sub>max</sub> values for different IP receptor agonists determined by  $\beta$ -arrestin recruitment assays in CHO-hIP cells (enzyme fragment complementation assay).

	EC <sub>50</sub> [ $\sigma$ g]	E <sub>max</sub> [SD]
ACT-333679	51 nM [1.8]	40 % [6 %]
selexipag	794 nM [1.4]	24 % [6 %]
beraprost	212 nM [1.6]	90 % [2 %]
iloprost	35 nM [1.7]	100 % [0 %]
treprostinil	186 nM [1.4]	67 % [10 %]

EC<sub>50</sub> values were derived using the individual curve-intrinsic maxima.  $\sigma$ g: geometric standard deviation. E<sub>max</sub>: maximal efficacy compared to that of iloprost. SD: arithmetic standard deviation. n=6 measurements.

**Table 3.** Plasma concentrations of ACT-333679 during continuous iv infusion of selezipag over 7 days in SHR.

Day	ACT-333679 plasma concentration (nM)
1	1518 ±269
3	2622 ±1274
6	797 ±94

Data presented as mean ± S.E.M. (n = 3)

**Table 4.** Plasma concentrations of treprostinil during continuous i.v. infusion over 48 hours in SHRs.

hours	treprostinil plasma concentration (nM)
4	28.6 ±3.2
8	27.3 ±1.6
24	25.1 ±5.1
48	25.5 ±7.4

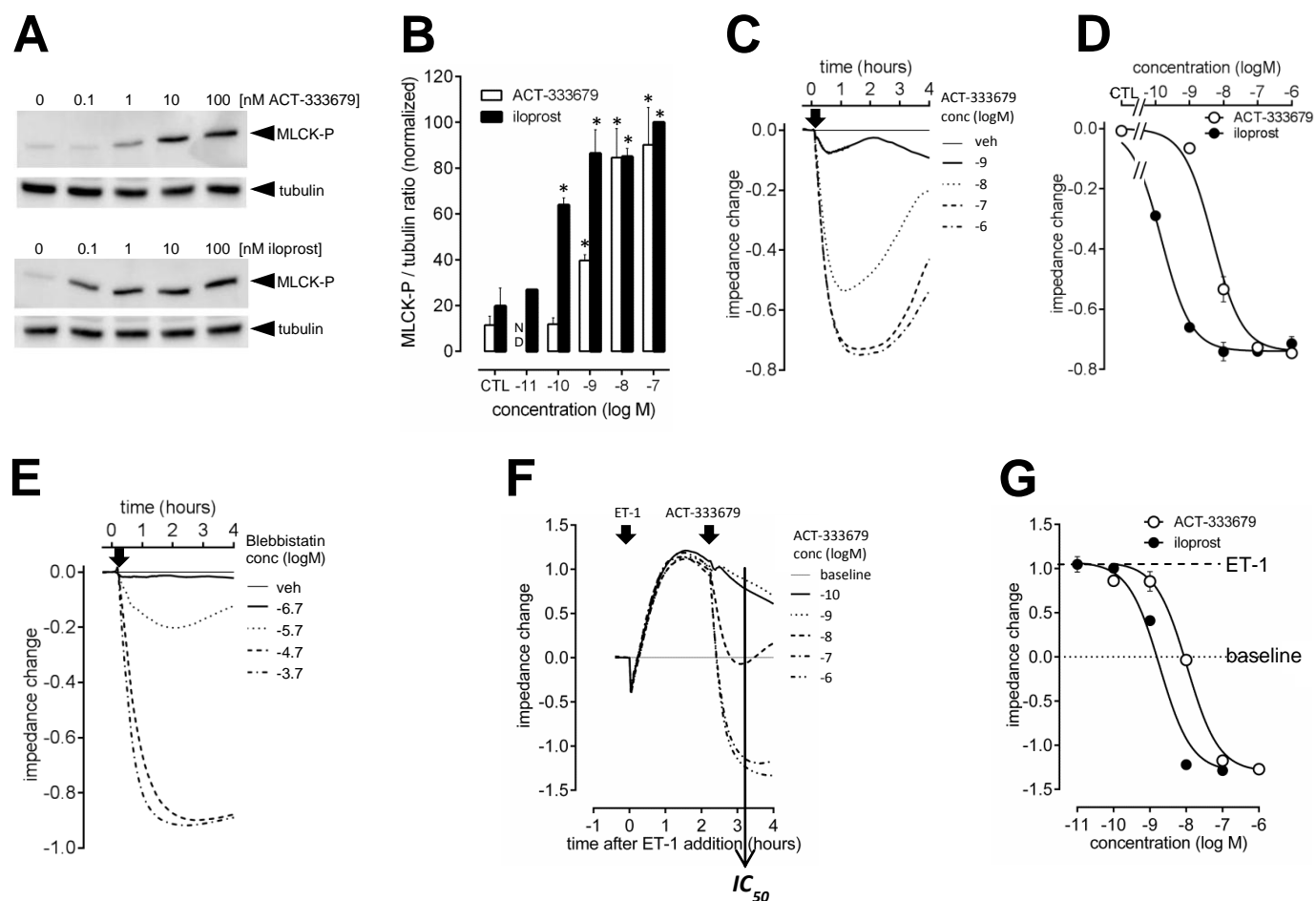
Data presented as mean ± S.E.M (n = 4)

Selexipag  
(parent compound)

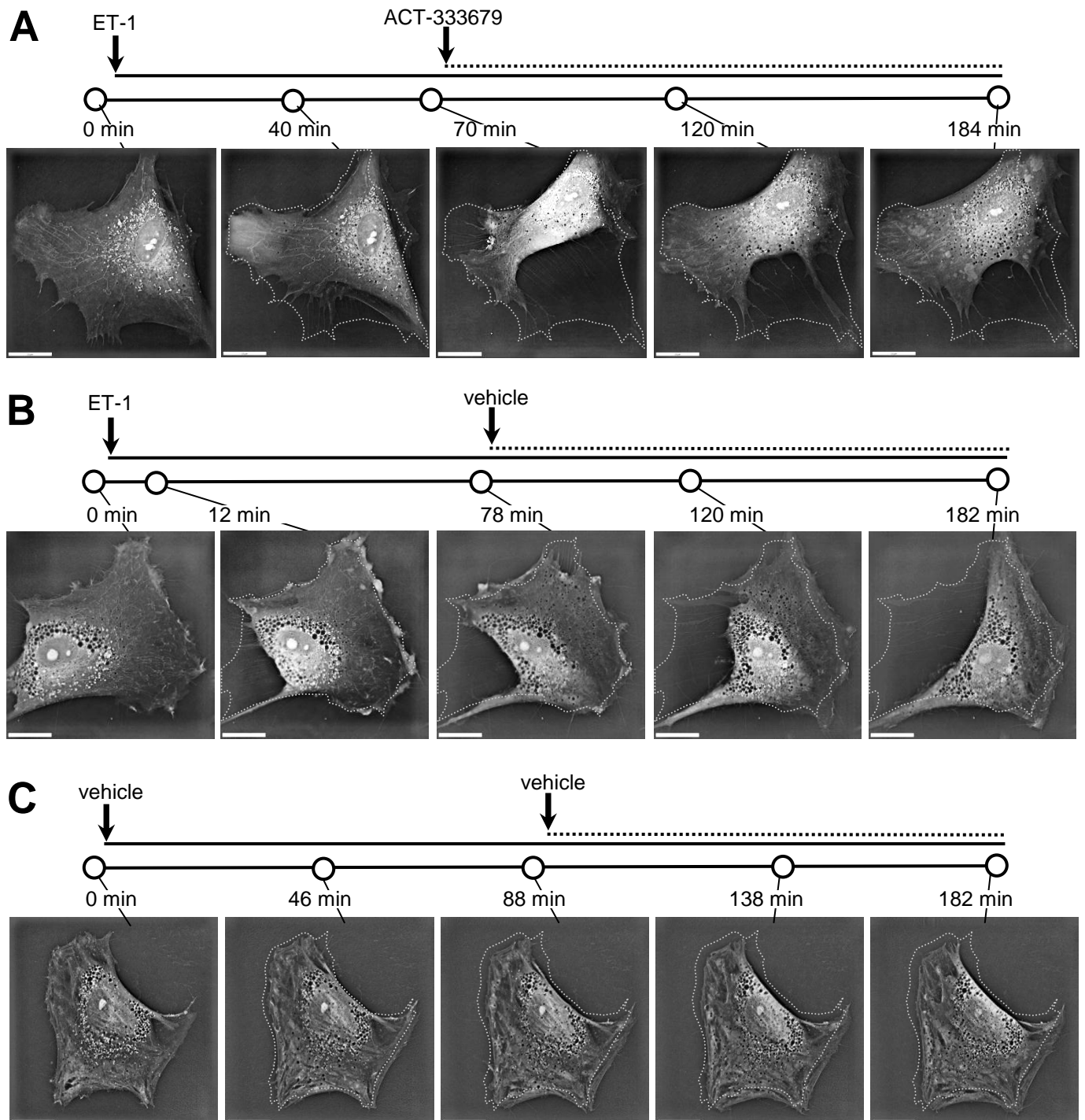
Hydrolysis

ACT-333679  
(active metabolite)

**Figure 2**



**Figure 3**



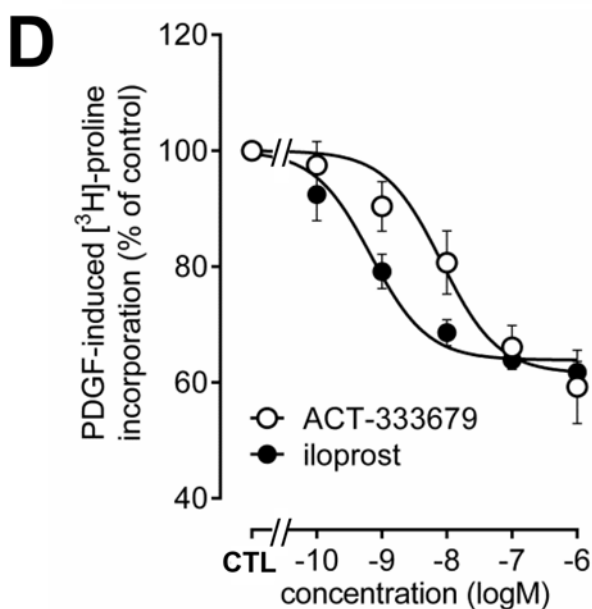
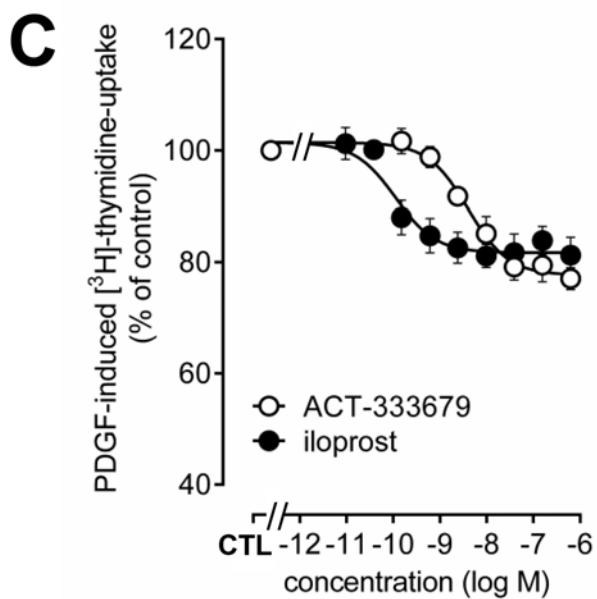
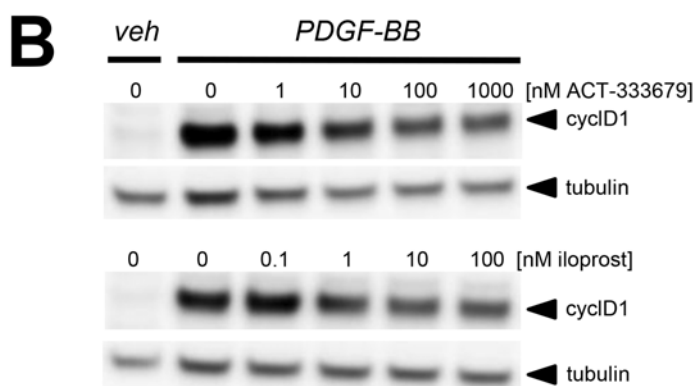
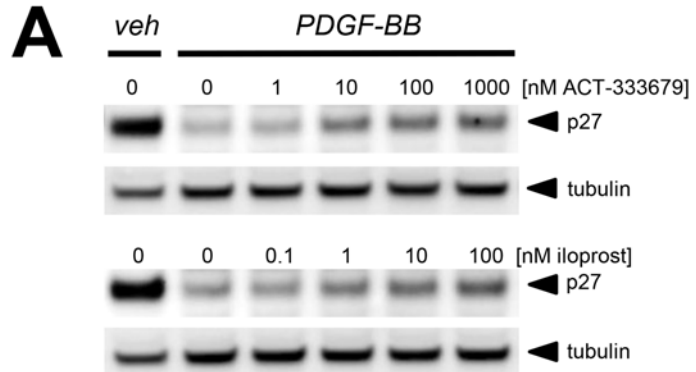


**Figure 5**

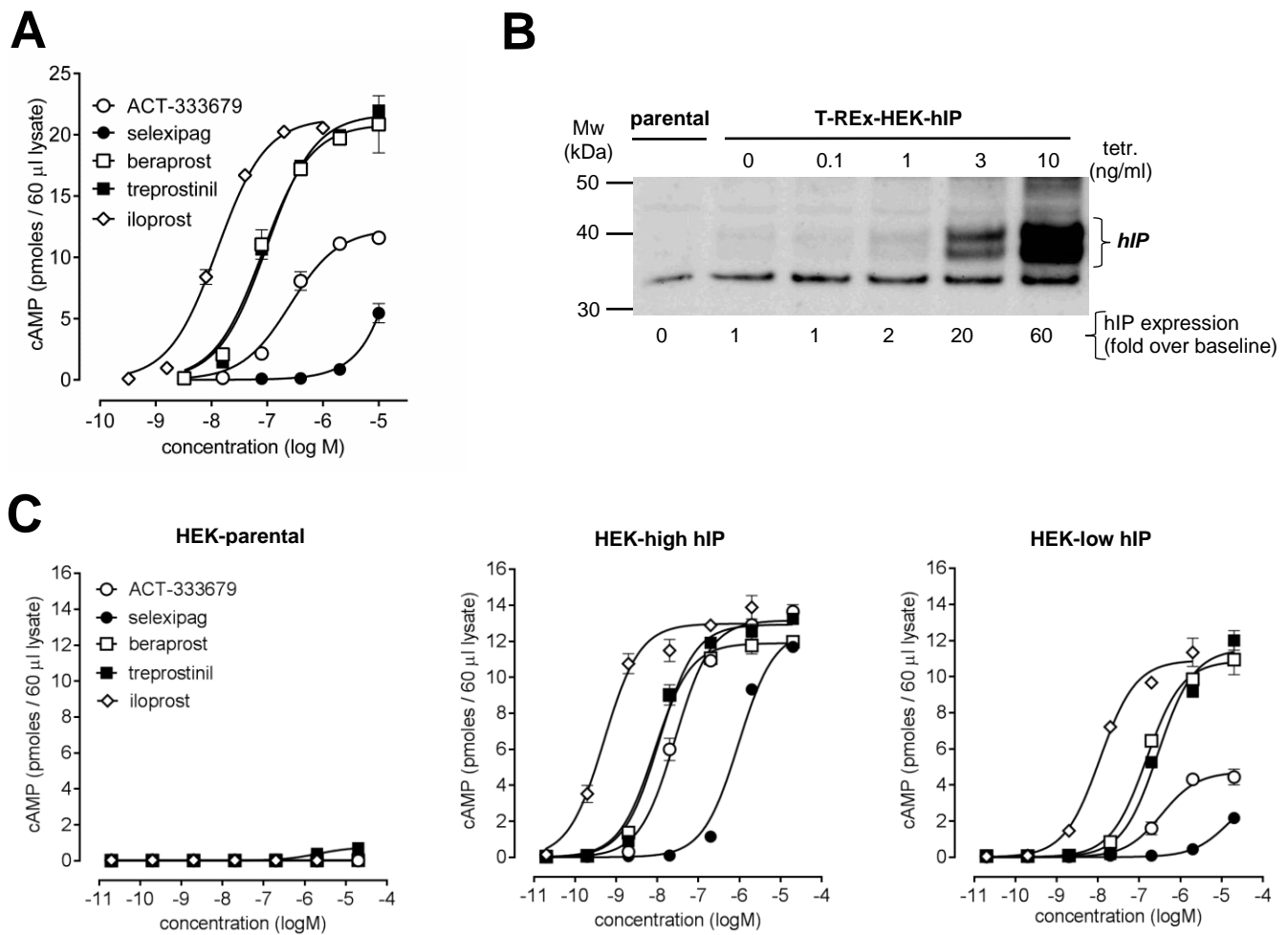


**Figure 6**

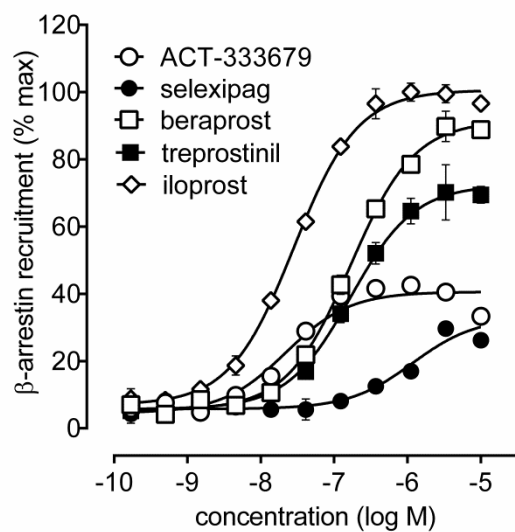


**Figure 7**

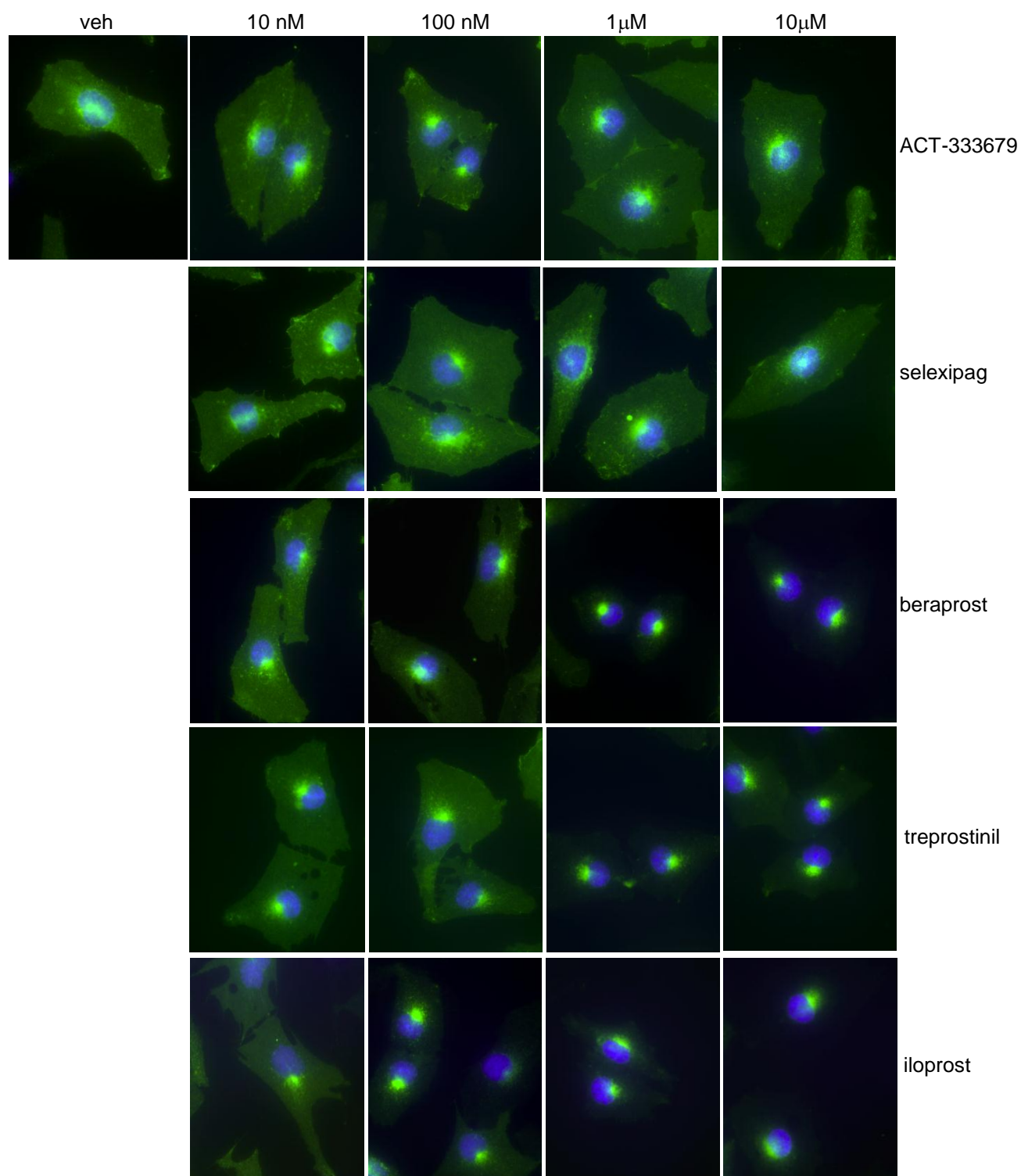


**Figure 8**

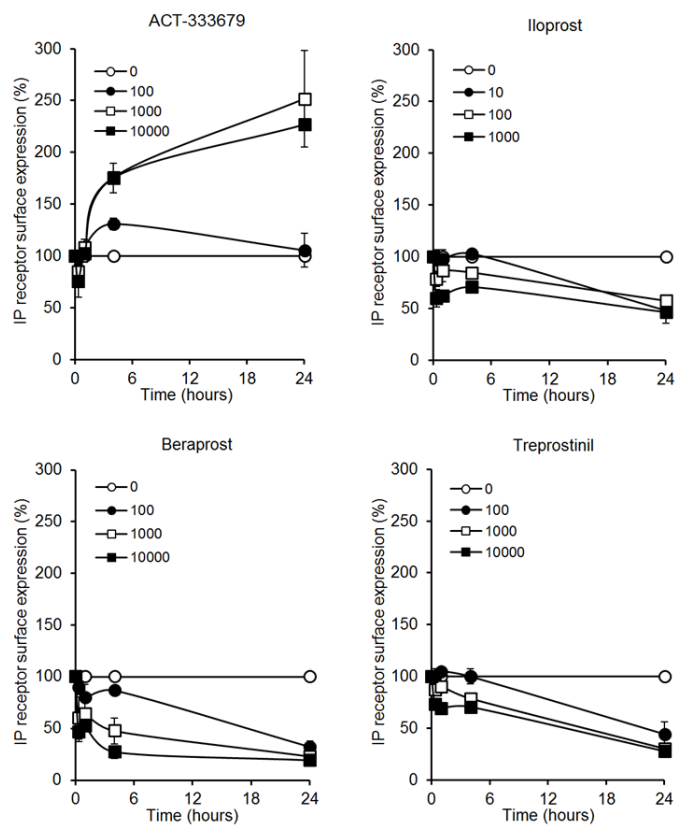


**Figure 9**

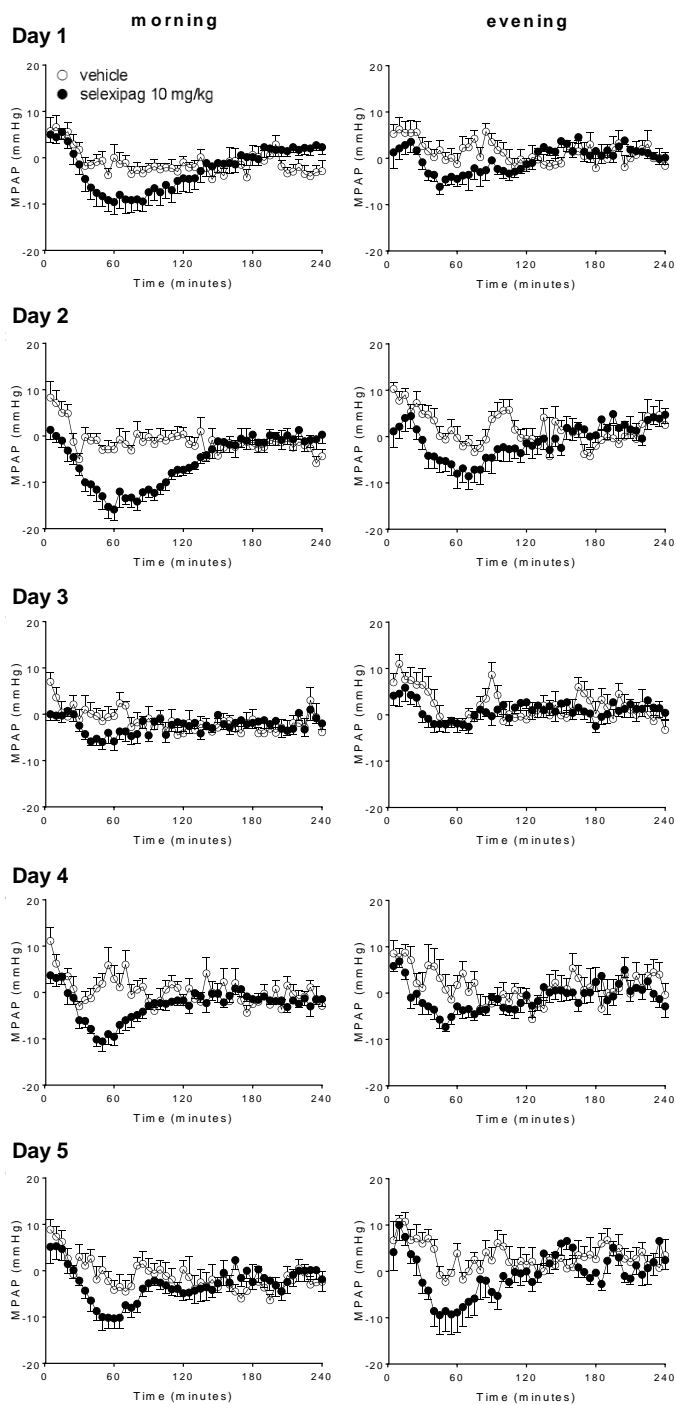


**Figure 10**

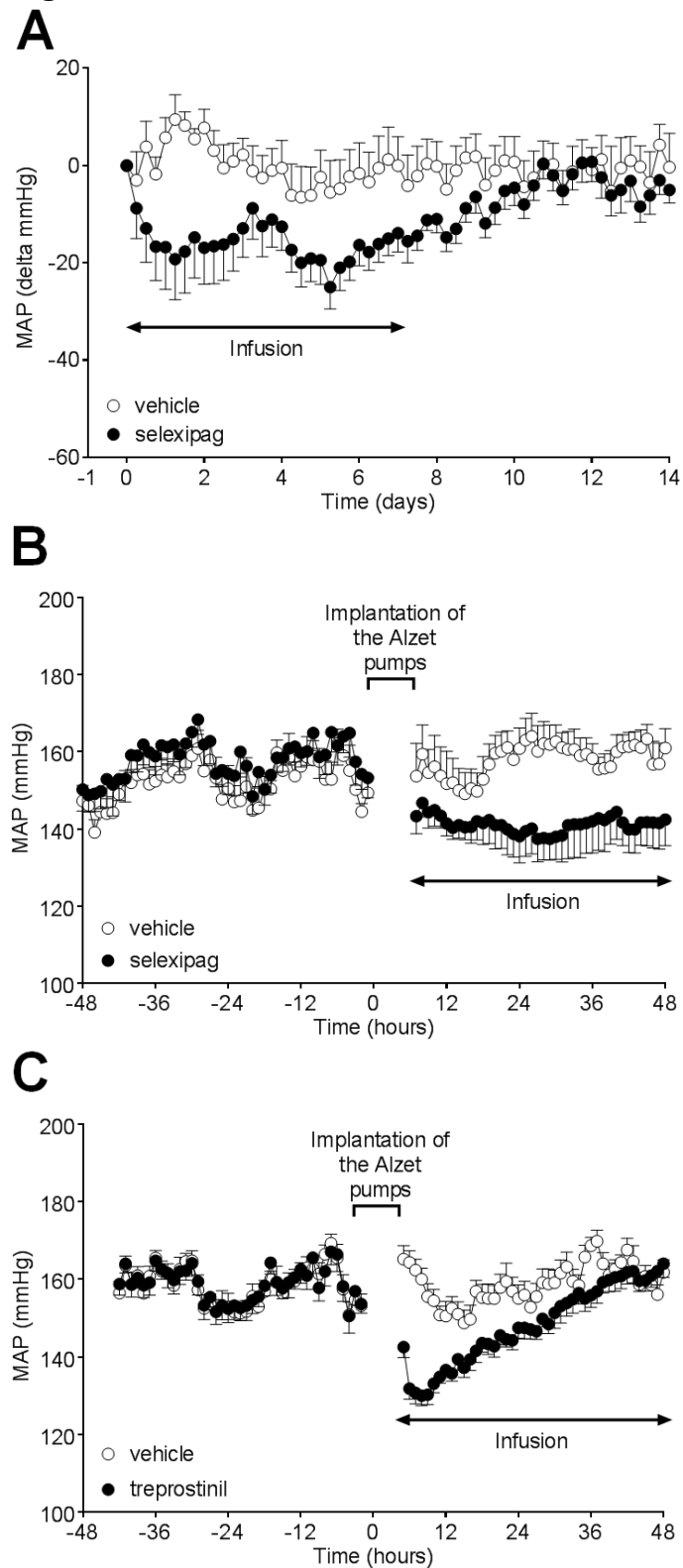


**Figure 11**

